Table 2 – PCR primers for detection of gene transcripts.

Name	Sequence	Size (bp)
Nanog	Forward: 5′ AGT CCC AAA GGC AAA CAA CCC ACT TC 3′ Reverse: 5′ ATC TGC TGG AGG CTG AGG TAT TTC TGT CTC 3′	164
Sox2	Forward: 5′ ACC GGC GGC AAC CAG AAG AAC AG 3′ Reverse: 5′ GCG CCG CGG CCG GTA TTT AT 3′	253
UTF1	Forward: 5′ ACC AGC TGC TGA CCT TGA AC 3′ Reverse: 5′ TTG AAC GTA CCC AAG AAC GA 3′	230
GAPDH	Forward: 5′ GCT CAG ACA CCA TGG GGA AGG T 3′ Reverse: 5′ GTG GTG CAG GAG GCA TTG CTG A 3′	474

Immunoblot analysis

Whole lysates of GBS6 or NCR-G3 cells were loaded on 10% SDS/PAGE (40 μg total protein/lane) and transferred to a nitrocellulose membrane. The blots were probed with antibodies against anti-Oct3/4 (C-20 for the C-terminus of OCT4/3 of human origin; sc-8629, Santa Cruz), developed with polyclonal rabbit anti-goat Immunoglobulins/HRP antibody (P0160; Dako), and detected by chemiluminescence following the manufacturer's protocol (ECL Western Blotting Analysis System, Amersham).

Flow cytometric analysis

Cells were stained for 30 min at 4 °C with primary antibodies and immunofluorescent secondary antibodies. The cells were then analyzed on a Cytomics FC 500 (Beckman Coulter, Inc., Fullerton, CA, USA) and the data were analyzed with the FC500 CXP Software ver.2.0 (Beckman Coulter, Inc., Fullerton, CA, USA). Antibodies against human CD9 (555372, PharMingen), CD13 (IM0778, Beckman), CD14 (6603511, Beckman), CD24 (555426, PharMingen), CD29 (6604105, PharMingen), CD31 (IM1431, Beckman), CD34 (IM1250, Beckman), CD44 (IM1219, Beckman), CD45 (556828, PharMingen), CD50 (IM1601, Beckman), CD55 (IM2725, Beckman), CD59 (IMK3457, Beckman), CD73 (550257, PharMingen), CD81 (555676, PharMingen), CD90 (IM1839, Beckman), CD105 (A07414, Beckman), CD106 (IM1244, Beckman), CD117 (IM1360, Beckman), CD130 (555756, PharMingen), CD133 (130-080-801, Miltenyi Biotec), CD135 (IM2234, Beckman), CD140a (556002, PharMingen), CD140b (558821, PharMingen), CD157 (D036-3, IBL), CD166 (559263, PharMingen), CD243 (IM2370, Beckman), ABCG2 (K0027-3, IBL),

Table 3 – Expression of human ES cell-associated genes.

A

Cell		OCT4/3	SOX2	NANOG	UTF1	TDGF1	ZIC3	DPPA4	MYC	KLF4
GBS6	Flags	P	A	A	A	A	A	A	P	A
	Raw	2493	56	9	15	23	19	9	3261	171
GBS6-5azaC	Flags	P	A	A	A	A	A	A	P	A
	Raw	6620	146	19	28	20	15	11	1359	102
NCR-G1	Flags	A	A	A	A	P	P	A	A	A
	Raw	46	67	11	19	5180	2349	97	157	91
NCR-G2	Flags	P	A	P	A	P	P	P	A	A
	Raw	2093	120	3972	166	2154	389	873	160	84
NCR-G3	Flags	P	P	P	P	P	P	P	P	P
	Raw	14338	1239	14925	9208	11207	5294	4036	1086	1151
NCR-G4	Flags	P	P	P	P	P	P	P	P	A
	Raw	10602	352	9469	1684	9830	2741	2138	746	151
H4-1	Flags	A	A	A	A	A	A	A	P	P
	Raw	83	13	11	17	40	7	2	1635	489
3F0664	Flags	A	A	A	A	A	A	A	P	P
	Raw	56	63	14	34	21	21	22	735	832
Yub10F	Flags	A	A	A	A	A	A	A	P	A
	Raw	19	49	9	63	12	12	4	680	9

B

Gene symbol	Probe set ID	Gene name
POU5F1	208286_x_at	Oct4/3
SOX2	213721_at	Sox2
NANOG	220184_at	Nanog; Nanog homeobox
UTF1	208275_x_at	Utf1; undifferentiated embryonic cell transcription factor 1
TDGF1	206286_s_at	Tdgf1; teratocarcinoma-derived growth factor 1
ZIC3	207197_at	Zic3; odd-paired homolog
DPPA4	219651_at	Dppa4; developmental pluripotency associated 4
MYC	202431_s_at	c-myc
KLF4	220266_s_at	Klf4; Kruppel-like factor 4

A. Gene expression was examined with the Human Genome U133A Probe array (Affymetrix). Raw data values (*Raw*) for each gene expression are shown. *Flags*: Gene expression was judged to be "*P* (present)" or "*A* (absent)" in each cell by the GeneChip Analysis Suite 5.0 computer program. GBS6-5azaC: GBS6 cells were exposed to 3 μM 5′-aza-2′-deoxycytidine for 24 h, and then cultured without any treatment for 24 h.
B. Gene names for each symbol.

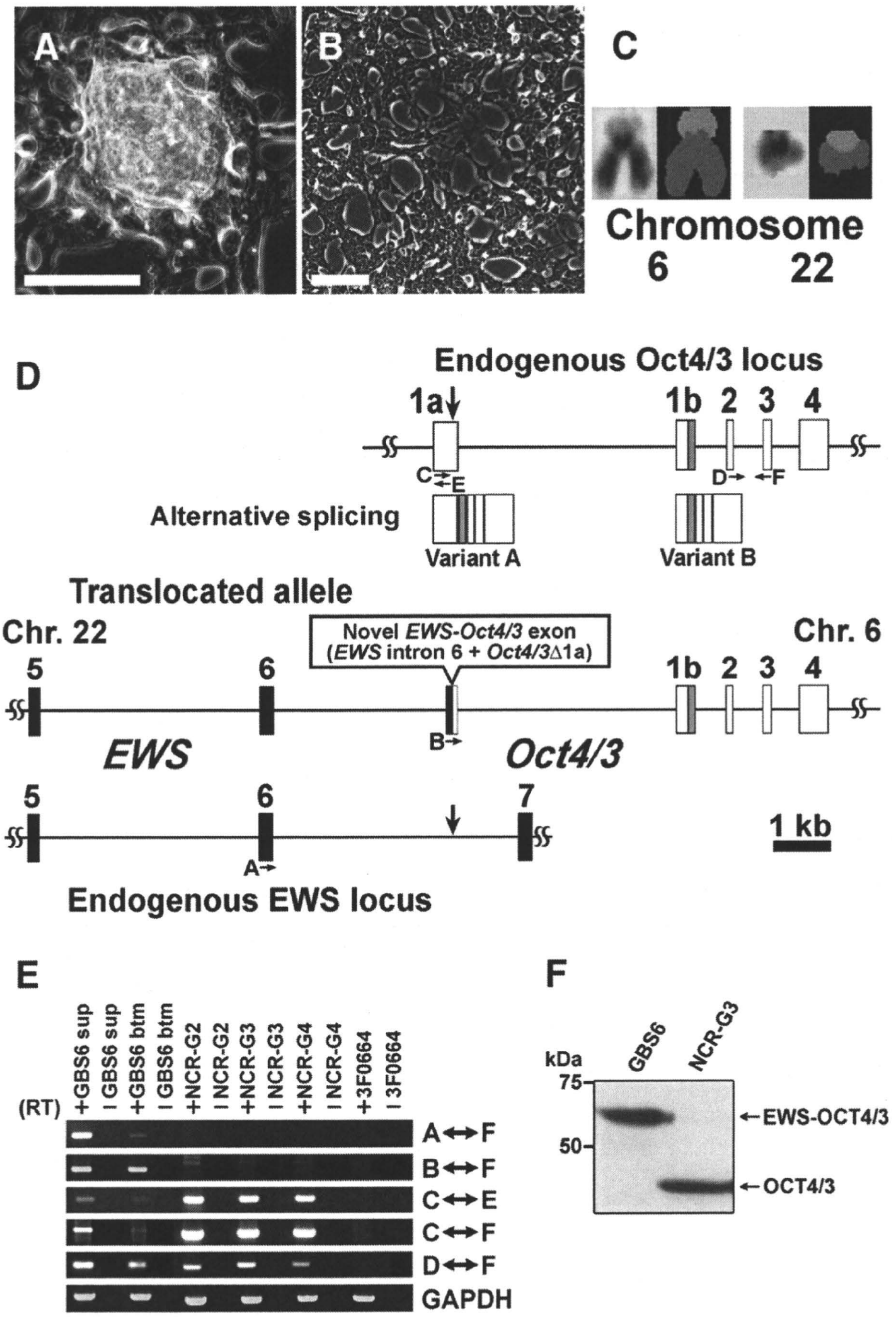

Fig. 1 – Phase contrast micrograph of GBS6 cells, and expression of the translocated *POU5F1/OCT4/3* gene. A cell line termed "GBS6" was generated from primary or first passage cells of a pelvic tumor [31]. (A) GBS6 cell aggregate (GBS6 sup). Scale bar: 100 μm. (B) GBS6 adherent cells (GBS6 btm). Scale bar: 100 μm. (C) G-banding karyotypic analysis and Spectral karyotyping (SKY) analysis of the translocated chromosomes. (D) Schematic representation of the *EWS-OCT4/3* structure in the t(6;22) tumor. *EWS* exons are represented by black boxes and *OCT4/3* exons by open boxes. The *OCT4/3*-1b exon is composed of an open and gray box. The novel *EWS-OCT4/3* chimeric exon is created by the fusion between *EWS* intron 6 and part of the exon of *OCT4/3* (Δ1a). The vertical arrows indicate each breakpoint on either chromosome 22 (*EWS*) or chromosome 6 (*OCT4/3*). The horizontal arrows indicate the position and direction of primers for PCR (Table 1). (E) RT-PCR analysis of the translocated *OCT4/3* gene and the untranslocated *OCT4/3* gene in GBS6 cell, NCR-G2, NCR-G3, NCR-G4, and 3F0664 cells. NCR-G2, NCR-G3, and NCR-G4 cells are embryonal carcinoma cells, and 3F0664 cells are mesenchymal cells. (F) Western blot analysis of EWS-OCT4/3 in GBS6 cells. Western blot analysis was performed using anti-Oct4/3 antibody. EWS-OCT4/3 chimeric protein (~58 kDa) was detected in GBS6 cells. The positions of prestained molecular markers (BIO-RAD) are indicated to the left (kDa).

HLA-ABC (IM1838, Beckman), HLA-DR, DP, DQ (6604366, Beckman), SSEA-1 (MAB4301, Chemicon), SSEA-3 (MAB4303, Chemicon), SSEA-4 (MAB4304, Chemicon), STRO-1 (MAB1038, R and D Systems), TRA-1-60 (MAB4360, Chemicon), and TRA-1-81 (MAB4381, Chemicon) were adopted as primary antibodies. PE-conjugated anti-mouse Ig antibody (550589, Pharmingen), PE-conjugated anti-mouse IgM antibody (555584, Pharmingen) and PE-conjugated anti-rat Ig antibody (550767, Pharmingen) were used as secondary antibodies. X-Mean, the sum of the intensity divided by total cell number, was automatically calculated, and it was adopted for the evaluation of this experiment.

Implantation of cells into mice

GBS6 cells ($>1\times10^7$) were subcutaneously inoculated into an immunodeficient, NOD/Shi-*scid*, IL-2Rγ^{null} mouse (NOG mouse) (CREA, Tokyo, Japan). Subcutaneous specimens were resected at 2 weeks after implantation. The operation protocols were accepted by the Laboratory Animal Care and the Use Committee of the National Research Institute for Child and Health Development, Tokyo (approval number: 2003-002 and 2005-003).

Immunohistochemistry analysis

Immunohistochemical analysis was performed as previously described [34–36] with antibodies to MIC2 (clone# 12E7, cat# M3601, DAKO, Carpinteria, CA, USA), vimentin (clone# V9, cat# M0725, DAKO, Carpinteria, CA, USA), neurofilament protein 70 kDa (NF-L, clone# 2F11, cat# M0762, DAKO, Carpinteria, CA, USA), desmin (clone# D9, cat# 010031, Bio-Science Products AG, Emmenbruecke, Switzerland), smooth muscle actin (clone# 1A4, cat# M0851, DAKO, Carpinteria, CA, USA), and OCT4/3 (clone# C-10, cat# sc-5279, Santa Cruz Biotechnology, Inc., CA, USA) in PBS containing 1% bovine serum albumin. As a methodological control, the primary antibody was omitted. Immunohistochemical analysis of iPS cells was performed according to the manufacturer's protocol [SCR002,

A

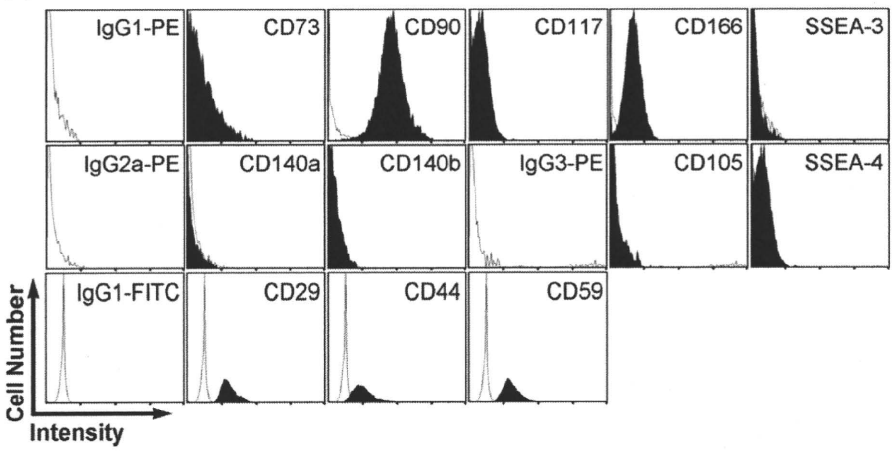

B

Negative (y≦0.1)			Low (0.1<y<1)	Positive (1<y)
CD13	CD106	ABCG2	CD73	CD9
CD14	CD117	HLA-DR,DQ,DP	CD166	CD29
CD24	CD130	SSEA-1		CD44
CD31	CD133	SSEA-3		CD59
CD34	CD135	SSEA-4		CD81
CD45	CD140a	Stro-1		CD90
CD50	CD140b	TRA-1-60		HLA-A,B,C
CD55	CD157	TRA-1-81		
CD105	CD243			

Fig. 2 – Cell surface marker analysis of GBS6 cells. (A) Flow cytometric analysis of cell surface markers in GBS6 cells. The results of CD73, CD90, CD117, CD166 and SSEA-3 were compared with the result of their isotype control, PE-conjugated IgG1. The results of CD140a and CD140b were compared with the result of PE-conjugated IgG2a. The results of CD105 and SSEA-4 were compared with the result of PE-conjugated IgG3. The results of CD29, CD44 and CD59 were compared with the result of FITC-conjugated IgG1. *X*-axis and *Y*-axis indicate the intensity and the cell number, respectively. (B) Summary of cell surface markers. "*y*" is "X-means" subtracted by 'a value of isotype control'; "$y<0.1$", "$0.1<y<1$", and "$1<y$" were determined "negative", "low" and "positive", respectively.

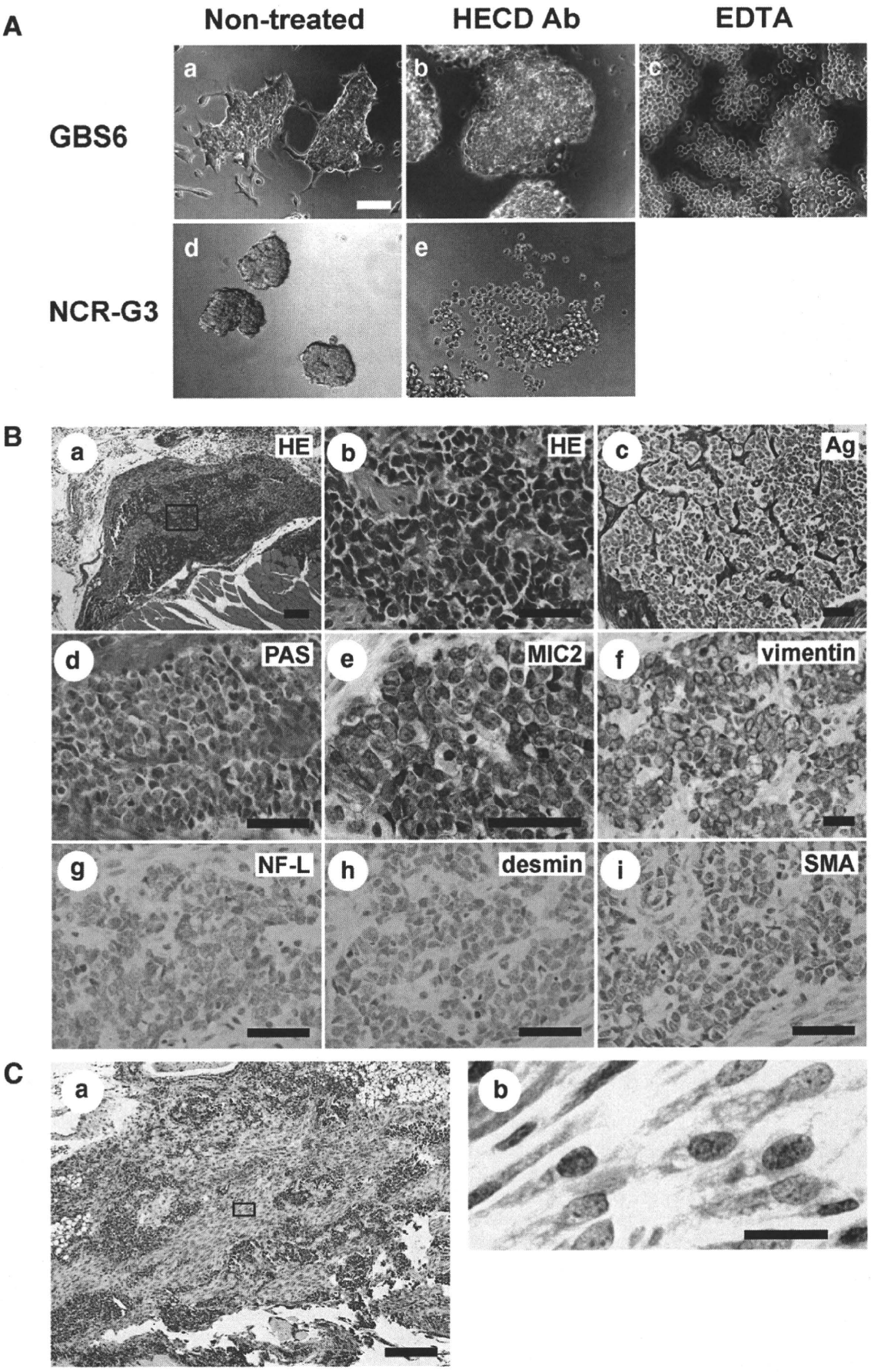
A
Non-treated
HECD Ab
EDTA
GBS6
NCR-G3
a
b
c
d
e
B
HE
HE
Ag
PAS
MIC2
vimentin
NF-L
desmin
SMA
C

Chemicon (Millipore)]. Primary antibodies included Oct-3/4 (C-10) (diluted at 1:300, sc-5279, Santa Cruz), NANOG (diluted at 1:300, RCAB0003P, ReproCELL), SSEA-4 (diluted at 1:300, MAB4304, CHEMICON), and TRA-1-60 (diluted at 1:300, MAB4360, CHEMICON). Secondary antibodies used were Alexa Fluor 546 Goat Anti-mouse IgG, 2 mg/mL (diluted at 1:300, A11003, Invitrogen), Alexa Fluor 488 Goat Anti-rabbit IgG, 2 mg/mL (diluted at 1:300, A11008, Invitrogen), and Alexa Fluor 488 Goat Anti-mouse IgG, 2 mg/mL, F (ab′)2 fragment (diluted at 1:300, A11017, Invitrogen). Nuclei were stained with 1 μg/mL DAPI (40043, Biotium).

Quantitative RT-PCR

RNA was extracted from cells using the RNeasy Plus Mini kit (Qiagen). An aliquot of total RNA was reverse transcribed by using an oligo (dT) primer. For the thermal cycle reactions, the cDNA template was amplified (ABI PRISM 7900HT Sequence Detection System) using the Platinum Quantitative PCR SuperMix-UDG with ROX (11743-100, Invitrogen) under the following reaction conditions: 40 cycles of PCR (95 °C for 15 s and 60 °C for 1 min) after an initial denaturation (95 °C for 2 min). Fluorescence was monitored during every PCR cycle at the annealing step. The authenticity and size of the PCR products were confirmed using a melting curve analysis (using software provided by Applied Biosystems) and a gel analysis. mRNA levels were normalized using *GAPDH* as a housekeeping gene. POU5F1-2-F and POU5F1-3-R primers were used to detect the *OCT4/3* gene (see Table 1, D and F).

Chromatin immunoprecipitation (ChIP) assays

Chromatin immunoprecipitation was performed according to the instructions of the EZ ChIP Chromatin Immunoprecipitation Kit (17-371, Upstate Biotechnology Inc., Chicago, IL, USA). Histone and DNA were cross-linked with 1% formaldehyde for 10 min at room temperature and formaldehyde was then inactivated by the addition of 125 mM glycine. The chromatin was then sonicated to an average DNA fragment length of 200 to 1000 bp. Soluble chromatin reacted with and without anti-acetylated Histone H3 (06-599, Upstate Biotechnology Inc., Chicago, IL, USA), and anti-acetylated Histone H4 (06-866, Upstate Biotechnology Inc., Chicago, IL, USA). The immunocomplex was purified and collected in elution buffer (0.1 M $NaHCO_3$, 1% sodium dodecyl sulfate). Crosslinking was then reversed using elution buffer containing RNase A (0.03 mg/mL) and NaCl (0.3 M) by incubation for 4 h at 65 °C. Supernatant obtained without antibody was used as the input control. The DNA was treated with proteinase K for 1 h at 45 °C and purified. For all ChIP experiments, quantitative PCR analyses were performed in real time as described in this manuscript. Relative occupancy values were calculated by determining the apparent immunoprecipitation efficiency (ratios of the amount of immunoprecipitated DNA to that of the input sample) and normalized to the level observed at a control region. For all the primers used, each gave a single product of the right size adult stem cell confirmed by agarose gel electrophoresis and dissociation curve analysis. These primers also gave no DNA product in the no-template control. The following three primer sets for human *OCT4/3*, as previously described [26], were adopted for real-time PCR to quantitate the ChIP-enriched DNA: human *POU5F1*-A (-2613/-2396), 5′-GGG GAACCTGGAGGATGG-CAAGCTGAGAAA-3′ and 5′-GGCCTGGTGGGGGTGGGAGG AACAT-3′; human *POU5F1*-B (-1779/-1563), 5-CCTGCACCCCTCCACAAATCACTC GC-3′ and 5′-TGCAATCCCCTCAAAGACTGAGCCTCAGAC-3′ ; human *POU5F1*-C (-237/-136), 5′-GAGGGGCGCCAGTTGTGTCTCCCGGTTTT-3′ and 5′-GGGAGGTGGG GGGAGAAACTGAGGCGAAGG-3′.

DNA methylation analysis

The NCR-G2 (JCRB cell bank number; JCRB1167) [32], NCR-G3 (JCRB cell bank number; JCRB1168) [32], GBS6, and Yub636BM (human bone marrow cells derived from an extra digit) cells were prepared for this assay. Genomic DNA was isolated using DNeasy Blood and Tissue Kit (69504, QIAGEN). Primers were selected from the CpG island regions with homogenous CpG site methylation patterns. The target region of the genes used for methylation analysis and the primer sequences used for PCR amplification are shown in Table 4. One of the two primers in the PCR amplification of the target regions is tagged with a T7 promoter sequence: cagtaatacgactcactatagggagaaggct. The PCR reactions were carried out in a total volume of 5 μL using 1 pmol of each primer, 40 μM dNTP, 0.1 U HotStar Taq DNA polymerase (QIAGEN), 1.5 mM $MgCl_2$, 5× PCR buffer (final concentration 1×), and bisulfite-converted DNA. The reaction mix was preactivated for 15 min at 95 °C. The reactions were amplified in 45 cycles of 95 °C for 20 s, 62 °C for 30 s, and 72 °C for 30 s followed by 72 °C for 3 min. Unincorporated dNTPs were dephosphorylated by adding 1.7 μL DNase-free water and 0.3 U Shrimp Alkaline Phosphatase (SAP). The reaction was incubated at 37 °C for 20 min and SAP was then heat-inactivated for 10 min at 85 °C. Typically, 2 μL of the PCR reaction was directly used as a template in a 6.5 μL combined transcription-cleavage reaction. Twenty units of T7 polymerase (Epicentre) were used to incorporate either dCTP or dTTP in the transcripts. Ribonucleotides at 1 mM and the dNTP substrate at 2.5 mM were used. RNase A (Sequenom) was included to cleave the in vitro transcript. The mixture was then further diluted with water to a final volume of 27 μL. Conditioning of the phosphate backbone prior to MALDI-TOF MS was achieved by the addition of 6 mg CLEAN resin (Sequenom). The cleavage reaction samples (15 nL) were dispensed onto silicon

Fig. 3 – In vitro and in vivo characteristics of GBS6 cells. (A) Ca++-dependent, E-cadherin-independent adhesion of GBS6 cell aggregates. GBS6 cells (a) were unaffected by the antibody to E-cadherin (b), but were dissociated by EDTA, Ca++ chelator (c). In contrast, NCR-G3 cells (d), serving as a control since they are E-cadherin-dependent, were dissociated and induced to death by the antibody to E-cadherin (e). Scale bar: 100 μm. (B) Immunohistochemical analysis of GBS6 cells implanted into the subcutaneous tissue of NOG mice. GBS6 cells at 2 weeks after implantation (a, b: hematoxylin and eosin stain, c: silver stain, d: PAS stain) were examined for immunohistochemical analysis using antibodies to MIC2 (e), vimentin (f), neurofilament protein 70 kDa (g: NF-L), desmin (h), and smooth muscle actin (i: SMA). Scale bars: 200 μm (a) and 50 μm (b–i). (C) Immunohistochemical analysis with the anti-OCT4/3 antibody of GBS6 cells implanted into the subcutaneous tissue of NOG mice. GBS6 cells at 2 weeks after implantation were examined for immunohistochemical analysis using antibodies to OCT4/3. The higher-magnification image of the region enclosed by a square in "a" (b). Scale bars: 200 μm (a) and 20 μm (b).

chips preloaded with matrix (SpectroCHIP, Sequenom). Mass spectra were collected using a MassARRAY mass spectrometer (Sequenom). Spectra were analyzed using proprietary peak picking and spectra interpretation tools (EpiTYPER, Sequenom).

For analysis of DNA methylation, we examined the methylation-dependent C/T sequence changes introduced by bisulfite treatment. Those C/T changes are reflected as G/A changes on the reverse strand and hence result in a mass difference of 16 kDa for

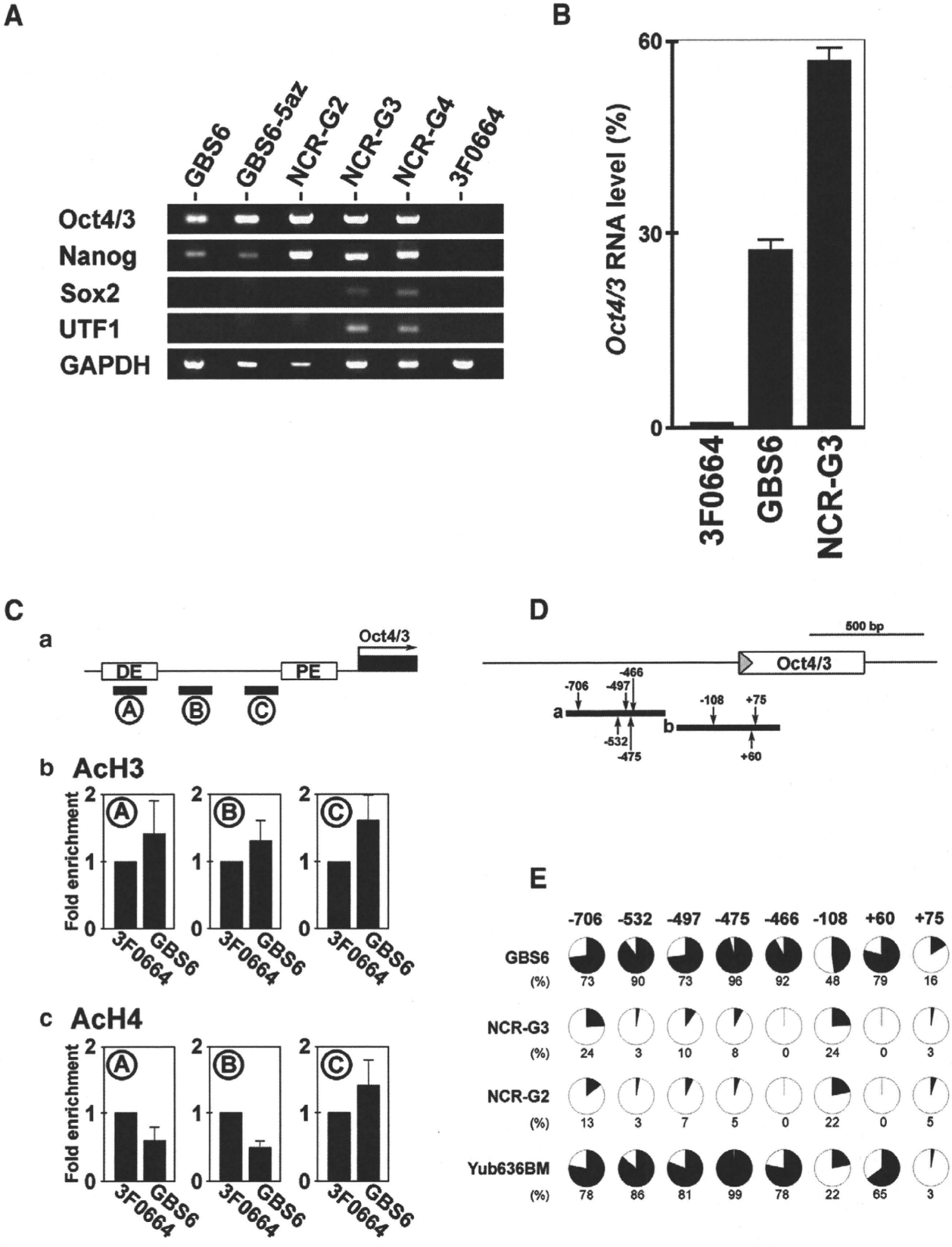

each CpG site enclosed in the cleavage products generated from the RNA transcript. The mass signals representing nonmethylated DNA and those representing methylated DNA, built signal pairs, which are representative for the CpG sites within the analyzed sequence substring. The intensities of the peaks were compared, and the relative amount of methylated DNA was calculated from this ratio. The method yields quantitative results for each of these sequence-defined analytic units referred to as CpG units, which contain either one individual CpG site or an aggregate of subsequent CpG sites.

Plasmid construction

Each open reading frame of human *OCT4/3* and *SOX2* was amplified by RT-PCR using the RNA extracted from NCR-G2 cells (JCRB cell bank number; JCRB1167) [32], a complex-type germ cell tumor cell line. Also, those of *c-MYC* and *KLF4* were amplified by RT-PCR using the RNA extracted from the bone marrow stromal cell line, UET13. A Gateway cassette composed of an attR1/R2 flanked CmR and ccdB (Invitrogen) was amplified by PCR and ligated into the Eco RI/Not I site of pMXs retroviral expression vector to create pMXs-DEST [37]. PCR amplification was performed by using KOD-Plus-DNA polymerase (KOD-201, TOYOBO). The constructs were confirmed by sequencing.

Retroviral infection and iPS cell generation

293FT cells (Invitrogen) were plated at 2×10^6 cells per 100 mm dish and incubated overnight. The next day, the cells were co-transfected with pMXs-OCT4/3, pMXs-SOX2, pMXs-c-MYC, pMXs-KLF4, pCL-GagPol, and pHCMV-VSV-G vectors with TransIT-293 reagent (Mirus, Madison, WI). Twenty-four hours after transfection, the medium was replaced with a new medium, which was collected after 48 h as the virus-containing supernatant. MRC-5 cells were seeded at 1×10^5 cells per 35 mm dish 1 day before infection. The virus-containing supernatants were filtered through a 0.45 μm pore-size filter, ultracentrifuged at 8500 rpm for 16 h, and then resuspended in DMEM (D6429, SIGMA) supplemented with 4 mg/mL polybrene (Nacalai Tesque). Equal amounts of concentrated supernatants containing each of the four retroviruses were mixed, transferred to MRC-5 cells, and incubated for 8 h. The MRC-5 cells were cultured for 4 days and replated on an irradiated MEF feeder layer in 100 mm dish. The medium was replaced with the iPSellon medium supplemented with 10 ng/mL bFGF. One-half of the medium was changed every day and the cells were cultured up to 30 days after a day of infection. Colonies were picked up and transferred into 0.2 mL of iPSellon medium when colonies appeared. The colonies were mechanically dissociated to small clumps by pipeting up and down or mechanically cut using a STEMPRO EZPassage disposable passaging tool (23181010, Invitrogen). The cell suspension was transferred on irradiated MEF feeder in 4-well plates [176740, Nunc (Thermo Fisher Scientific)]. We define this stage as passage 1.

Teratoma formation

iPS cells were harvested by accutase treatment, collected into tubes, and centrifuged, and the pellets were suspended in the iPSellon medium. The same volume of Basement Membrane Matrix (354234, BD Biosciences) was added to the cell suspension. Cells (1×10^7) were implanted subcutaneously to a BALB/c-*nu/nu* mouse (CREA, Japan) for 4 weeks. Tumors were dissected and fixed with PBS containing 4% paraformaldehyde. Paraffin-embedded tissue was sliced and stained with hematoxylin and eosin.

GeneChip expression analysis

Total RNA was extracted from cells using the RNeasy Mini Kit (74104, Qiagen, Valencia, CA). Genomic DNA was eliminated by DNase I (2215A, TAKARA BIO INC.) treatments. From all RNA samples, 5 μg of total RNA was used as a starting material for the microarray sample preparation. Double-stranded cDNA was synthesized from DNase-treated total RNA, and the cDNA was subjected to in vitro transcription in the presence of biotinylated nucleoside triphosphates using the Enzo BioArray HighYield RNA Transcript Labeling Kit (Enzo Life Sciences, Inc., Farmingdale, NY), according to the manufacturer's protocol (One-Cycle Target Labeling and Control Reagent package). Human-genome-wide gene expression was examined with the Human Genome U133A Probe array (GeneChip, Affymetrix), which contains the oligonucleotide probe set for approximately 23,000 full-length genes and expressed sequence tags (ESTs), according to the manufacturer's protocol (Expression Analysis Technical Manual and GeneChip small sample target labeling Assay Version 2 technical note, http://www.affymetrix.com/support/technical/index.affx) as previously described [5]. Hierarchical clustering and principle component

Fig. 4 – Expression of the *OCT4/3* gene and histone modification of the *OCT4/3* promoter in GBS6 cells. (A) Expression of embryonic stem cell-enriched genes in GBS6, NCR-G2, NCR-G3, NCR-G4, and 3F0664 cells. GBS6 cells expressed the *OCT4/3* and *NANOG* genes, but not the *SOX2* and *UTF1* genes. NCR-G2 cells expressed the *OCT4/3* and *NANOG* genes; both NCR-G3 cells and NCR-G4 cells expressed the *OCT4/3*, *NANOG*, *SOX2* and *UTF1* genes. 3F0664 mesenchymal cells did not express these four kinds of embryonic stem cell-enriched genes. POU5F1-1a-F and POU5F1-1a-R (Table 1) were used to amplify the endogenous *OCT4/3* gene. (B) Quantitative PCR analysis to assess the expression level of *OCT4/3* mRNA in GBS6. *OCT4/3* mRNA level is expressed relative to 3F0664 cells control. (C) Real-time PCR to quantitate the ChIP-enriched DNA using acetylated Histone H3 and acetylated Histone H4 antibodies. Schematic of the location of the amplicons (A–C) used to detect ChIP-enriched fragments in *OCT4/3* shown relative to the distal enhancer (DE)/CR4 region, to the proximal enhancer (PE), and to transcription start site (arrow) (a). The relative levels of acetylated Histone H3 (b) and acetylated Histone H4 (c) modifications were detected in GBS6 cells and 3F0664 cell control. GBS6 cells are represented by black bars and 3F0664 cells by open bars. (D) DNA methylation analysis in the promoter region of the *OCT4/3* gene. The target regions of *OCT4/3* used for the quantitative DNA methylation analysis. Region 'a' and Region 'b' include 5 (−706, −532, −497, −475, −466) and 3 (−108, +60, +75) CpG sites, respectively. The positions of CpG sites are relative to the *OCT4/3* transcription start site (gray triangle). (E) The relative amount of methylated DNA ratio (%) at each CpG site is indicated as the black area in the pie chart.

analysis were performed to group mesenchymal cells obtained from bone marrow into subcategories (http://lgsun.grc.nia.nih.gov/ANOVA/).

Results

Establishment of human cells of mesenchymal origin with overexpression of the translocated POU5F1/OCT4/3 gene

To investigate whether cells of mesenchymal origin acquire an embryonic phenotype, a novel human cell line termed GBS6 was established from the pelvic bone tumor, of which histology shows diffuse proliferation of undifferentiated tumor cells with oval nuclei and scant but short spindle cytoplasm [31]. The generated cells grew attached to the dish as a polygonal cell sheet with cell aggregates forming in the center (Figs. 1A, B), and retained the reciprocal translocation, t(6; 22), detected in the original tumor (Fig. 1C). The *EWS-OCT4/3* chimeric gene expression also remained (Figs. 1D, E and Table 1). Embryonal carcinoma (EC) cells, i.e., NCR-G2, NCR-G3, and NCR-G4, served as control cells expressing the endogenous *OCT4/3* gene. Immunoblot analysis revealed that EWS-OCT4/3 fusion protein was expressed in GBS6 cells (Fig. 1F).

Cell surface markers of GBS6 cells

GBS6 cell surface markers were evaluated by flow cytometric analysis (Fig. 2). The results showed that GBS6 cells were strongly positive (Positive; Fig. 2B) for CD9, CD29 (integrin β1), CD44, CD59, CD81, CD90 (Thy-1) and HLA-A,B,C (HLA class I); weakly positive (Low; Fig. 2B) for CD73 and CD166 (ALCAM); negative (Negative; Fig. 2B) for CD55, CD105 (endogrin), CD140a (PDGFRα), and CD140b (PDGFRβ). The lack of CD13, CD55, CD105, CD106, CD140a, and CD140b in GBS6 cells suggests that the surface markers of GBS6 cells are different from those of conventional mesenchymal cells [10,38,39].

E-cadherin-independent growth of GBS6 cells

To investigate whether GBS6 cells survive dependent on E-cadherin-like human embryonic cells, the cells were treated by an inhibitory antibody to E-cadherin (HECD Ab) and EDTA (Fig. 3A). GBS6 cell survival was unaffected by the E-cadherin antibody but affected by EDTA (Fig. 3A-a, b, c). In contrast, NCR-G3 cells, human embryonal carcinoma cells that proliferate in an E-cadherin-dependent manner, were dissociated and induced to apoptosis by the E-cadherin antibody (Fig. 3A-d, e).

Implantation of GBS6 cells into immunodeficient mice

To investigate an in vivo phenotype of GBS6 cells, the cells were intramuscularly injected into immunodeficient NOG mice and examined by histopathology and immunohistochemistry (Fig. 3B). The injected cells exhibited an undifferentiated phenotype with oval nuclei and scant spindle cytoplasm (Fig. 3B-b), and showed an alveolar configuration (Fig. 3B-c). The cells were negative by the PAS stain (Fig. 3B-d). The cells were immunohistochemically positive for MIC2 and vimentin (Fig. 3B-e, f), and negative for neurofilament, desmin, and smooth muscle actin (Fig. 3B-g, h, i). The cells retained OCT4/3 in their nuclei even after implantation (Fig. 3C).

Expression of ES-enriched genes

To determine if GBS6 cells express ES cell-enriched genes, that is, the *OCT4/3*, *NANOG*, *SOX2*, and *UTF1* genes, RT-PCR with specific primer sets (Table 2) and gene chip analyses were performed. GBS6 cells expressed the endogenous *OCT4/3* and *NANOG* genes like NCR-G2, NCR-G3, and NCR-G4 embryonal carcinoma cells, but did not express the *SOX2* and *UTF1* genes (Fig. 4A). The results of the RT-PCR analysis were compatible with those of the gene chip analysis (GSE8113, Table 3). To compare the expression level of stem cell-specific genes in GBS6 cells, ES cells, and mesenchymal cells, we performed a quantitative RT-PCR analysis. The expression level of *OCT4/3* was about half that of human EC cells, but was more than twenty-five times that of 3F0664 mesenchymal cells (Fig. 4B). The results show that the expression level of *OCT4/3* is comparable to that of human EC cell.

To determine if the cis-regulatory element of the *OCT4/3* gene has so-called open chromatin structure, we performed the chip analysis using antibodies to acetylated H3 and acetylated H4 (Fig. 4C). The results show that acetylated histone levels which the *OCT4/3* promoter is wrapped around in GBS6 cells are comparable with those in 3F0664 mesenchymal cells. We also performed methylation analysis of the *OCT4/3* gene in GBS6 cells because the expression of *OCT4/3* gene is regulated by methylation (Figs. 4D, E and Table 4). The promoter region of the *OCT4/3* gene was heavily methylated in GBS6 cells as compared with human NCR-G3 embryonal carcinoma cells expressing the *OCT4/3* gene at a high level.

Cell reprogramming assay

To investigate if chimeric EWS-OCT4/3 induces iPS cells like native OCT4/3, we performed Yamanaka's reprogramming assay on MRC-5 human fetal lung fibroblasts (Fig. 5A), using the chimeric *EWS-OCT4/3* construct with the *KLF-4*, *SOX2*, and *c-MYC* genes according to the conventional protocol [40] with some modifications. We failed to obtain iPS cells using the *EWS-OCT4/3*, *KLF-4*, *SOX2*, and *c-MYC* constructs (Fig. 5B), albeit trials of three independent experiments, whereas, for a control, we successfully generated 101 clones of iPS cells from MRC-5 cells using the *OCT4/3*, *KLF-4*, *SOX2*, and *c-MYC* constructs (Fig. 5C). The iPS cells generated from MRC-5 cells expressed human ES cell-specific surface antigens (Figs. 5D–G). In vivo implantation analysis showed that iPS cells generated various tissues including neural tissues (Fig. 5H: ectoderm), cartilage (Fig. 5I: mesoderm),

Table 4 – Primers used for PCR amplification of the bisulfite-converted DNA.

Name	Sequence	Size (bp)
Region 'a'	Forward: 5′ TTG GTT ATT GTG TTT ATG GTT GTT G 3′	437
	Reverse: 5′ TAA ACC AAA ACA ATC CTT CTA CTC C 3′	
Region 'b'	Forward: 5′ TTT GGG TAA TAA AGT GAG ATT TTG TTT 3′	452
	Reverse: 5′ CTA ACC CTC CAA AAA AAC CTT AAA A 3′	

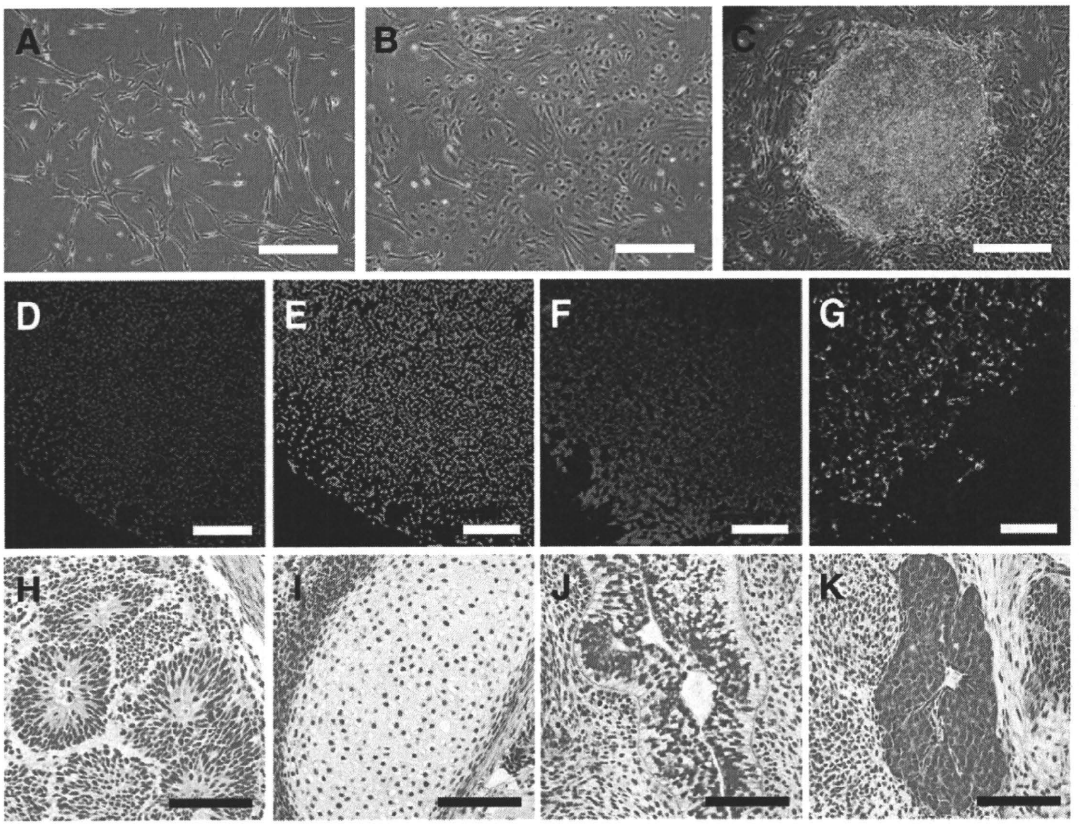

Fig. 5 – Induction of iPS cells from MRC-5 cells and teratoma formation. (A) Morphology of MRC-5 cells. (B) Morphology of cells using *EWS-OCT4/3*, *KLF-4*, *SOX2*, and *c-MYC* genes at Day 30 after infection. (C) Morphology of established iPS cell (clone 16: Fetch) colony using *OCT4/3*, *KLF-4*, *SOX2*, and *c-MYC* genes at Day 20 after infection. (D–G) Immunocytochemistry for OCT4/3 (D), NANOG (E), SSEA-4 (F), and TRA-1-60 (G). Nuclei were stained with DAPI. Bars = 500 μm (A–C), and 200 μm (D–G). In addition, chromosomal G-band analyses showed that human iPS cells from MRC-5 had a normal karyotype of 46XY (not shown). The analysis of short tandem repeat shows that novel iPS cells from MRC-5 cells were not a result of cross-contamination. Hematoxylin and eosin staining of teratoma derived from the generated iPS cells. Cells (1×10^7) were implanted subcutaneously to a BALB/c-*nu/nu* mouse for 4 weeks. Histological examination showed that the tumor contained various tissues, neural tissues (H; ectoderm), cartilage (I; mesoderm), a gut-like epithelial tissue (J; endoderm), and a hepatic tissue (K; endoderm). Bars = 100 μm (H–K).

a gut-like epithelial tissue (Fig. 5J: endoderm), and a hepatic tissue (Fig. 5K: endoderm). These results imply that the chimeric *EWS-OCT4/3* gene does not participate in reprogramming of somatic cells.

Principle component analysis of global gene expression in GBS6 cells

To determine whether GBS6 cells are categorized into embryonal cells or mesenchymal cells, global gene expression patterns of GBS6 cells, embryonal carcinoma cells (NCR-G2, NCR-G3, and NCR-G4), yolk sac tumor cells (NCR-G1), and marrow stromal cells (3F0664, H4-1, and Yub10F) were further analyzed by principle component analysis (PCA), which reduces high-dimensionality data into a limited number of principle components (Fig. 6). The first principle component (PC1) captures the largest contributing factor of variation, which characterizes the differential expression of genes. As we were interested in the differential gene expression component, we plotted the position of each cell type against the PC1, PC2, and PC3 axis in three-dimensional space by using virtual reality modeling language (Fig. 6A). Close examination of the 3D model identified PC1 as the most representative view of the 3D model. PC1 axis direction is therefore used to characterize the differential gene expression (Fig. 6B). In addition, hierarchical analysis of the cells analyzed for global gene expression revealed that GBS6 cells are categorized into embryonal carcinoma cells and yolk sac tumor cells, i.e., NCR-G1, -G2, -G3, and -G4 cells (Fig. 6C).

Discussion

In this study, we generated a cell line with a transitional form between mesenchymal cells and embryonic stem cells. Loss of mesenchyme-specific cell markers, i.e., CD13, CD55, CD105, CD106, CD140a and CD140b, and modification of cell survival with the calcium chelator indicate that GBS6 cells are no longer mesenchymal cells. Global and drastic differences in gene expression with the GeneChip analysis support the conclusion that GBS6 cells no longer exhibit the profile of mesenchymal cells. It is also noteworthy that this transition phenotype is reliably inherited ex vivo after a series of in vitro passages.

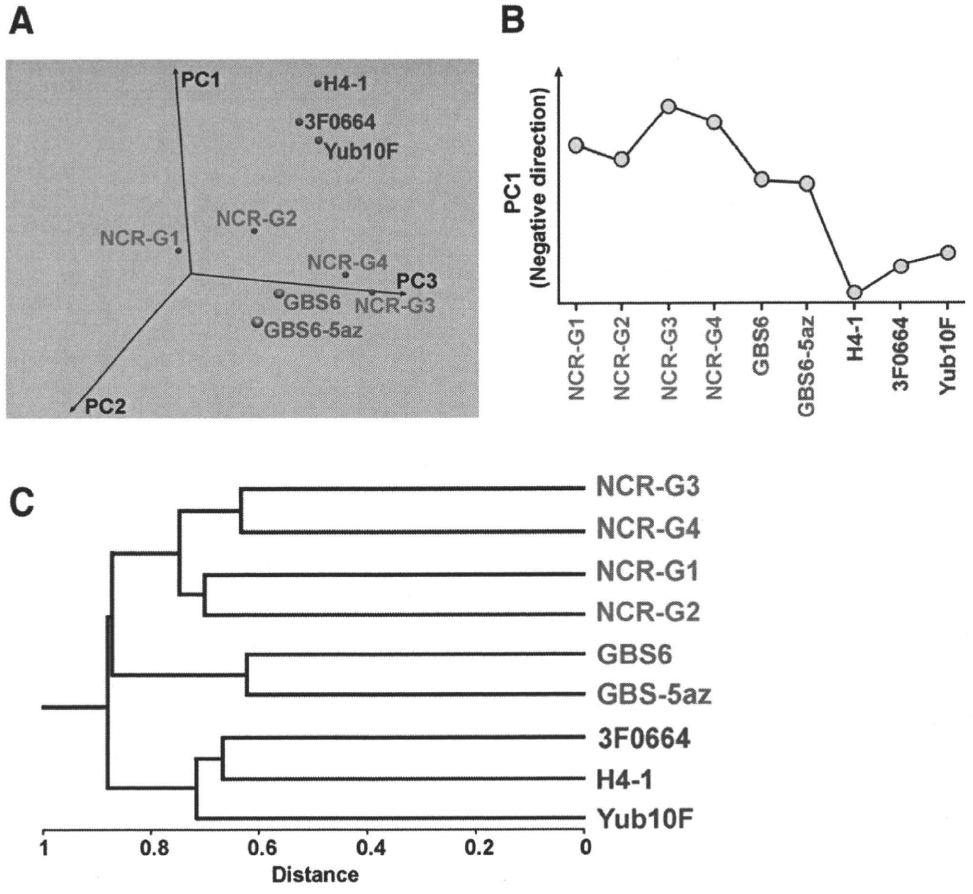

Fig. 6 – Principal component analysis and hierarchical clustering of gene expression in GBS6 cells, embryonal carcinoma cells, and bone marrow cells. (A) 3D-representation of principle component analysis. (B) Principal components of PC1 axis, negative direction. (C) Hierarchical clustering analysis of averages.

OCT4/3 function and its physiological partner EWS in embryonic transition

ES-like cells or iPS cells are generated from murine fibroblasts by transfecting four genes, i.e., *OCT4/3*, *SOX2*, *KLF-4* and *c-MYC* are necessary for the mesenchymal–embryonic transition [1–3]. However, OCT4/3 alone is not sufficient to confer embryonic phenotypes to human bone marrow-derived cells, NIH3T3 cells (data not shown) or embryonic fibroblasts [1]. EWS and OCT4/3 are directly bound both in vitro and in vivo [41]; in other words, EWS is a binding partner of OCT4/3. Therefore, the EWS-OCT4/3 protein in GBS6 cells is considered a fusion between physiological partners. EWS and OCT4/3 are co-expressed in the pluripotent mouse and human ES cells. To investigate if the EWS-OCT4/3 has a transcriptional activity, we performed the luciferase assay. The results show that the chimeric *EWS-OCT4/3* gene has comparable or higher transcriptional activity than the native *OCT4/3* gene does (Supplementary Fig. S1). Ectopic expression of non-chimeric EWS enhances the transactivation activity of OCT4/3; the N-terminal QSY domain of EWS and the C-terminal POU domain function as a transcriptional activation and DNA binding, respectively [42,43]. The *OCT4/3* gene is overexpressed under the cis-regulatory element of the *EWS* gene [31], and the functional co-operation of OCT4/3 and EWS at a protein level to transcriptional activation may lead to embryonic transformation in GBS6 cells. Converting mesenchymal cells to embryonic cells opposes the usual direction of ES cell differentiation [44]; and this is achieved by chimeric OCT4/3 with physiological co-activator EWS driven by the potent cis-regulatory element of the *EWS* gene [31]. This phenotypic conversion requires the molecular reprogramming of mesenchymal cells with new instructions.

Mesenchymal to embryonic "incomplete" transition by overexpression of chimeric OCT4/3

OCT4/3 fused to *EWS* not only participates in oncogenesis [29,31], but also contributes to mesenchymal–embryonic transition, at least in part from the viewpoint of global gene expression profiles and cell surface markers (Figs. 2 and 6). GBS6 cells are subcategorized into groups of cells derived from testicular germ cell tumors (Fig. 6A, cells with embryonic phenotypes are shown in pink), and the PC1 axis indicates transition from mesenchymal cell group to embryonal cell group (Fig. 6B). This transition was, however, incomplete; some of the ES-specific genes were not reactivated. OCT4/3 is a member of the POU family of transcription factors, is expressed in pluripotent ES cells, including primordial germ cells [17–21], and functions as a master switch in differentiation by regulating cells that have, or can develop, pluripotent

potential. However, tight chromatin structure in GBS6 cells may render OCT4/3 recognition sequences inaccessible [45]. The OCT4/3 recognition sequences have been found in the cis-regulatory elements of the FGF-4 and CD140a/platelet-derived growth factor receptor-α gene [46], but GBS6 cells are indeed negative for CD140a (Fig. 2B). Alternatively, the lack of other essential transcription factors such as SOX2 and UTF1 (Fig. 4A, Table 3) and/or co-factors may be a cause of "incomplete" transition. Interestingly, this transition phenotype is reliably inherited ex vivo after a series of in vitro passages, and this may also be attributed to the function of OCT4/3 that is critical for self-renewal of embryonic stem cells [24].

Mesenchymal to epithelial transition is observed in physiological and pathological conditions [47–50]. In contrast, mesenchymal–embryonic transition has been achieved in an artificial experimental condition in vitro [1–3]. Homogenous positive staining for OCT4/3 in embryonal carcinoma cells supports the model that the encoded protein is crucial, and the absence of OCT4/3 in non-embryonal carcinoma cells is in agreement with the inability to generate pluripotent stem cells [51]. The cell line generated in this study with overexpression of chimeric OCT4/3, although this is just one case of rare human immortalized cells, provides us with insight into cell plasticity involving OCT4/3 that is essential for ES cell maintenance and into the complexity required for changing cellular identity.

Acknowledgments

We would like to express our sincere thanks to Michiyo Nasu for histological analysis, Yoriko Takahashi for data mining, and Kayoko Saito for secretary work. This study was supported by grants from the Ministry of Education, Culture, Sports, Science and Technology (MEXT) of Japan and Health and Labor Sciences Research Grants; by Research on Health Science Focusing on Drug Innovation from the Japan Health Science Foundation; by the Program for Promotion of Fundamental Studies in Health Science of the Pharmaceuticals and Medical Devices Agency; by the grant from Terumo Life Science Foundation; by a research Grant for Cardiovascular Disease from the Ministry of Health, Labor and Welfare; and by a Grant for Child Health and Development from the Ministry of Health, Labor and Welfare.

Appendix A. Supplementary data

Supplementary data associated with this article can be found, in the online version, at doi:10.1016/j.yexcr.2009.06.016.

REFERENCES

[1] K. Takahashi, S. Yamanaka, Induction of pluripotent stem cells from mouse embryonic and adult fibroblast cultures by defined factors, Cell 126 (2006) 663–676.
[2] K. Okita, T. Ichisaka, S. Yamanaka, Generation of germline-competent induced pluripotent stem cells, Nature 448 (2007) 313–317.
[3] M. Wernig, A. Meissner, R. Foreman, T. Brambrink, M. Ku, K. Hochedlinger, B.E. Bernstein, R. Jaenisch, In vitro reprogramming of fibroblasts into a pluripotent ES-cell-like state, Nature 448 (2007) 318–324.
[4] M.J. Go, C. Takenaka, H. Ohgushi, Forced expression of Sox2 or Nanog in human bone marrow derived mesenchymal stem cells maintains their expansion and differentiation capabilities, Exp. Cell Res. 314 (2008) 1147–1154.
[5] T. Mori, T. Kiyono, H. Imabayashi, Y. Takeda, K. Tsuchiya, S. Miyoshi, H. Makino, K. Matsumoto, H. Saito, S. Ogawa, M. Sakamoto, J. Hata, A. Umezawa, Combination of hTERT and bmi-1, E6, or E7 induces prolongation of the life span of bone marrow stromal cells from an elderly donor without affecting their neurogenic potential, Mol. Cell. Biol. 25 (2005) 5183–5195.
[6] R.H. Lee, B. Kim, I. Choi, H. Kim, H.S. Choi, K. Suh, Y.C. Bae, J.S. Jung, Characterization and expression analysis of mesenchymal stem cells from human bone marrow and adipose tissue, Cell. Physiol. Biochem. 14 (2004) 311–324.
[7] J.G. Toma, M. Akhavan, K.J. Fernandes, F. Barnabe-Heider, A. Sadikot, D.R. Kaplan, F.D. Miller, Isolation of multipotent adult stem cells from the dermis of mammalian skin, Nat. Cell Biol. 3 (2001) 778–784.
[8] C.H. Cui, T. Uyama, K. Miyado, M. Terai, S. Kyo, T. Kiyono, A. Umezawa, Menstrual blood-derived cells confer human dystrophin expression in the murine model of duchenne muscular dystrophy via cell fusion and myogenic transdifferentiation, Mol. Biol. Cell 18 (2007) 1586–1594.
[9] O.K. Lee, T.K. Kuo, W.M. Chen, K.D. Lee, S.L. Hsieh, T.H. Chen, Isolation of multipotent mesenchymal stem cells from umbilical cord blood, Blood 103 (2004) 1669–1675.
[10] M. Terai, T. Uyama, T. Sugiki, X.K. Li, A. Umezawa, T. Kiyono, Immortalization of human fetal cells: the life span of umbilical cord blood-derived cells can be prolonged without manipulating p16INK4a/RB braking pathway, Mol. Biol. Cell 16 (2005) 1491–1499.
[11] X. Zhang, A. Mitsuru, K. Igura, K. Takahashi, S. Ichinose, S. Yamaguchi, T.A. Takahashi, Mesenchymal progenitor cells derived from chorionic villi of human placenta for cartilage tissue engineering, Biochem. Biophys. Res. Commun. 340 (2006) 944–952.
[12] E.H. Allan, P.W. Ho, A. Umezawa, J. Hata, F. Makishima, M.T. Gillespie, T.J. Martin, Differentiation potential of a mouse bone marrow stromal cell line, J. Cell. Biochem. 90 (2003) 158–169.
[13] H. Imabayashi, T. Mori, S. Gojo, T. Kiyono, T. Sugiyama, R. Irie, T. Isogai, J. Hata, Y. Toyama, A. Umezawa, Redifferentiation of dedifferentiated chondrocytes and chondrogenesis of human bone marrow stromal cells via chondrosphere formation with expression profiling by large-scale cDNA analysis, Exp. Cell Res. 288 (2003) 35–50.
[14] S. Makino, K. Fukuda, S. Miyoshi, F. Konishi, H. Kodama, J. Pan, M. Sano, T. Takahashi, S. Hori, H. Abe, J. Hata, A. Umezawa, S. Ogawa, Cardiomyocytes can be generated from marrow stromal cells in vitro, J. Clin. Invest. 103 (1999) 697–705.
[15] N. Nishiyama, S. Miyoshi, N.M. Hida, T. Uyama, K. Okamoto, Y. Ikegami, K. Miyado, K. Segawa, M. Terai, M. Sakamoto, S. Ogawa, A. Umezawa, The significant cardiomyogenic potential of human umbilical cord blood-derived mesenchymal stem cells in vitro, Stem Cells 25 (2007) 2017–2024.
[16] J. Deng, B.E. Petersen, D.A. Steindler, M.L. Jorgensen, E.D. Laywell, Mesenchymal stem cells spontaneously express neural proteins in culture and are neurogenic after transplantation, Stem Cells 24 (2006) 1054–1064.
[17] H.R. Scholer, G.R. Dressler, R. Balling, H. Rohdewohld, P. Gruss, Oct-4: a germline-specific transcription factor mapping to the mouse t-complex, EMBO J. 9 (1990) 2185–2195.
[18] K. Okamoto, H. Okazawa, A. Okuda, M. Sakai, M. Muramatsu, H. Hamada, A novel octamer binding transcription factor is differentially expressed in mouse embryonic cells, Cell 60 (1990) 461–472.
[19] M.H. Rosner, M.A. Vigano, K. Ozato, P.M. Timmons, F. Poirier, P.W. Rigby, L.M. Staudt, A POU-domain transcription factor in early

stem cells and germ cells of the mammalian embryo, Nature 345 (1990) 686–692.
[20] M.F. Pera, D. Herszfeld, Differentiation of human pluripotent teratocarcinoma stem cells induced by bone morphogenetic protein-2, Reprod. Fertil. Dev. 10 (1998) 551–555.
[21] T. Goto, J. Adjaye, C.H. Rodeck, M. Monk, Identification of genes expressed in human primordial germ cells at the time of entry of the female germ line into meiosis, Mol. Hum. Reprod. 5 (1999) 851–860.
[22] M. Pesce, X. Wang, D.J. Wolgemuth, H. Scholer, Differential expression of the Oct-4 transcription factor during mouse germ cell differentiation, Mech. Dev. 71 (1998) 89–98.
[23] J. Nichols, B. Zevnik, K. Anastassiadis, H. Niwa, D. Klewe-Nebenius, I. Chambers, H. Scholer, A. Smith, Formation of pluripotent stem cells in the mammalian embryo depends on the POU transcription factor Oct4, Cell 95 (1998) 379–391.
[24] H. Niwa, J. Miyazaki, A.G. Smith, Quantitative expression of Oct-3/4 defines differentiation, dedifferentiation or self-renewal of ES cells, Nat. Genet. 24 (2000) 372–376.
[25] B. Abdel-Rahman, M. Fiddler, D. Rappolee, E. Pergament, Expression of transcription regulating genes in human preimplantation embryos, Hum. Reprod. 10 (1995) 2787–2792.
[26] J.L. Chew, Y.H. Loh, W. Zhang, X. Chen, W.L. Tam, L.S. Yeap, P. Li, Y.S. Ang, B. Lim, P. Robson, H.H. Ng, Reciprocal transcriptional regulation of Pou5f1 and Sox2 via the Oct4/Sox2 complex in embryonic stem cells, Mol. Cell. Biol. 25 (2005) 6031–6046.
[27] O. Delattre, J. Zucman, B. Plougastel, C. Desmaze, T. Melot, M. Peter, H. Kovar, I. Joubert, P. de Jong, G. Rouleau, A. Aurias, G. Thomas, Gene fusion with an ETS DNA-binding domain caused by chromosome translocation in human tumours, Nature 359 (1992) 162–165.
[28] F. Urano, A. Umezawa, W. Hong, H. Kikuchi, J. Hata, A novel chimera gene between EWS and E1A-F, encoding the adenovirus E1A enhancer-binding protein, in extraosseous Ewing's sarcoma, Biochem. Biophys. Res. Commun. 219 (1996) 608–612.
[29] F. Mitelman, B. Johansson, F. Mertens, The impact of translocations and gene fusions on cancer causation, Nat. Rev. Cancer 7 (2007) 233–245.
[30] M. Kuroda, T. Ishida, M. Takanashi, M. Satoh, R. Machinami, T. Watanabe, Oncogenic transformation and inhibition of adipocytic conversion of preadipocytes by TLS/FUS-CHOP type II chimeric protein, Am. J. Pathol. 151 (1997) 735–744.
[31] S. Yamaguchi, Y. Yamazaki, Y. Ishikawa, N. Kawaguchi, H. Mukai, T. Nakamura, EWSR1 is fused to POU5F1 in a bone tumor with translocation t(6;22)(p21;q12), Genes Chromosomes Cancer 43 (2005) 217–222.
[32] J. Hata, J. Fujimoto, E. Ishii, A. Umezawa, Y. Kokai, Y. Matsubayashi, H. Abe, S. Kusakari, H. Kikuchi, T. Yamada, T. Maruyama, Differentiation of human germ cell tumor cells in vivo and in vitro. Acta Histochem. Cytochem. 25 (1992) 563–576.
[33] E. Schrock, T. Veldman, H. Padilla-Nash, Y. Ning, J. Spurbeck, S. Jalal, L.G. Shaffer, P. Papenhausen, C. Kozma, M.C. Phelan, E. Kjeldsen, S.A. Schonberg, P. O'Brien, L. Biesecker, S. du Manoir, T. Ried, Spectral karyotyping refines cytogenetic diagnostics of constitutional chromosomal abnormalities, Hum. Genet. 101 (1997) 255–262.
[34] M. Sano, A. Umezawa, H. Abe, A. Akatsuka, S. Nonaka, H. Shimizu, M. Fukuma, J. Hata, EAT/mcl-1 expression in the human embryonal carcinoma cells undergoing differentiation or apoptosis, Exp. Cell Res. 266 (2001) 114–125.
[35] S. Gojo, N. Gojo, Y. Takeda, T. Mori, H. Abe, S. Kyo, J. Hata, A. Umezawa, In vivo cardiovasculogenesis by direct injection of isolated adult mesenchymal stem cells, Exp. Cell Res. 288 (2003) 51–59.
[36] T. Sugimoto, A. Umezawa, J. Hata, Neurogenic potential of Ewing's sarcoma cells, Virchows Arch. 430 (1997) 41–46.
[37] Y. Miyagawa, H. Okita, H. Nakaijima, Y. Horiuchi, B. Sato, T. Taguchi, M. Toyoda, Y.U. Katagiri, J. Fujimoto, J. Hata, A. Umezawa, N. Kiyokawa, Inducible expression of chimeric EWS/ETS proteins confers Ewing's family tumor-like phenotypes to human mesenchymal progenitor cells, Mol. Cell. Biol. 28 (2008) 2125–2137.
[38] B.L. Yen, H.I. Huang, C.C. Chien, H.Y. Jui, B.S. Ko, M. Yao, C.T. Shun, M.L. Yen, M.C. Lee, Y.C. Chen, Isolation of multipotent cells from human term placenta, Stem Cells 23 (2005) 3–9.
[39] E.K. Waller, J. Olweus, F. Lund-Johansen, S. Huang, M. Nguyen, G.R. Guo, L. Terstappen, The "common stem cell" hypothesis reevaluated: human fetal bone marrow contains separate populations of hematopoietic and stromal progenitors, Blood 85 (1995) 2422–2435.
[40] K. Takahashi, K. Tanabe, M. Ohnuki, M. Narita, T. Ichisaka, K. Tomoda, S. Yamanaka, Induction of pluripotent stem cells from adult human fibroblasts by defined factors, Cell 131 (2007) 861–872.
[41] J. Lee, B.K. Rhee, G.Y. Bae, Y.M. Han, J. Kim, Stimulation of Oct-4 activity by Ewing's sarcoma protein, Stem Cells 23 (2005) 738–751.
[42] D. Zhang, A.J. Paley, G. Childs, The transcriptional repressor ZFM1 interacts with and modulates the ability of EWS to activate transcription, J. Biol. Chem. 273 (1998) 18086–18091.
[43] S.L. Palmieri, W. Peter, H. Hess, H.R. Scholer, Oct-4 transcription factor is differentially expressed in the mouse embryo during establishment of the first two extraembryonic cell lineages involved in implantation, Dev. Biol. 166 (1994) 259–267.
[44] T. Barberi, L.M. Willis, N.D. Socci, L. Studer, Derivation of multipotent mesenchymal precursors from human embryonic stem cells, PLoS Med. 2 (2005) e161.
[45] H. Kimura, M. Tada, N. Nakatsuji, T. Tada, Histone code modifications on pluripotential nuclei of reprogrammed somatic cells, Mol. Cell. Biol. 24 (2004) 5710–5720.
[46] H.J. Kraft, S. Mosselman, H.A. Smits, P. Hohenstein, E. Piek, Q. Chen, K. Artzt, E.J. van Zoelen, Oct-4 regulates alternative platelet-derived growth factor alpha receptor gene promoter in human embryonal carcinoma cells, J. Biol. Chem. 271 (1996) 12873–12878.
[47] R. Kalluri, E.G. Neilson, Epithelial–mesenchymal transition and its implications for fibrosis, J. Clin. Invest. 112 (2003) 1776–1784.
[48] C. Martinez-Alvarez, M.J. Blanco, R. Perez, M.A. Rabadan, M. Aparicio, E. Resel, T. Martinez, M.A. Nieto, Snail family members and cell survival in physiological and pathological cleft palates, Dev. Biol. 265 (2004) 207–218.
[49] H. Peinado, F. Portillo, A. Cano, Transcriptional regulation of cadherins during development and carcinogenesis, Int. J. Dev. Biol. 48 (2004) 365–375.
[50] E. de Laplanche, K. Gouget, G. Cleris, F. Dragounoff, J. Demont, A. Morales, L. Bezin, C. Godinot, G. Perriere, D. Mouchiroud, H. Simonnet, Physiological oxygenation status is required for fully differentiated phenotype in kidney cortex proximal tubules, Am. J. Physiol. Renal Physiol. 291 (2006) F750–760.
[51] L.H. Looijenga, H. Stoop, H.P. de Leeuw, C.A. de Gouveia Brazao, A.J. Gillis, K.E. van Roozendaal, E.J. van Zoelen, R.F. Weber, K.P. Wolffenbuttel, H. van Dekken, F. Honecker, C. Bokemeyer, E.J. Perlman, D.T. Schneider, J. Kononen, G. Sauter, J.W. Oosterhuis, POU5F1 (OCT3/4) identifies cells with pluripotent potential in human germ cell tumors, Cancer Res. 63 (2003) 2244–2250.

THE JOURNAL OF GENE MEDICINE
J Gene Med 2008; **10**: 498–507.
Published online 18 February 2008 in Wiley InterScience (www.interscience.wiley.com) **DOI:** 10.1002/jgm.1171

RESEARCH ARTICLE

Efficient adenovirus vector-mediated PPAR gamma gene transfer into mouse embryoid bodies promotes adipocyte differentiation

Katsuhisa Tashiro[1,2]
Kenji Kawabata[1]
Haruna Sakurai[1,2]
Shinnosuke Kurachi[1,2]
Fuminori Sakurai[1]
Koichi Yamanishi[2,3]
Hiroyuki Mizuguchi[1,2]*

[1]*Laboratory of Gene Transfer and Regulation, National Institute of Biomedical Innovation, Osaka, Japan*

[2]*Graduate School of Pharmaceutical Sciences, Osaka University, Osaka, Japan*

[3]*National Institute of Biomedical Innovation, Osaka, Japan*

*Correspondence to:
Hiroyuki Mizuguchi, Laboratory of Gene Transfer and Regulation, National Institute of Biomedical Innovation, 7-6-8 Saito-Asagi, Ibaraki, Osaka 567-0085, Japan.
E-mail: mizuguch@nibio.go.jp

Received: 23 October 2007
Revised: 27 December 2007
Accepted: 7 January 2008

Abstract

Background Establishment of a transient gene delivery system, such as adenovirus (Ad) vectors, into embryonic stem (ES) cells and their aggregation form, embryoid bodies (EBs), is essential for its application in regenerative medicine because the transgene should not be integrated in the host genome. In this study, we optimized Ad vector-mediated transduction into EBs, and examined whether Ad vector-mediated transduction of adipogenesis-related gene into EBs could promote the adipocyte differentiation.

Methods We prepared β-galactosidase-expressing Ad vectors under the control of four different promoters (cytomegalovirus (CMV), rouse sarcoma virus, human elongation factor-1α, and CMV enhancer/β-actin promoter (CA)) to estimate the transduction efficiency. Adipocyte differentiation efficiency by transduction of the PPAR gamma or C/EBP alpha gene into EBs was examined.

Results Of the four promoters tested, the CA promoter exhibited the highest transduction efficiency in the EBs. However, Ad vector-mediated transduction was observed only in the periphery of the EBs. When repeated transduction by Ad vector was performed, gene expression was observed even in the interior of EBs as well. When EB-derived single cells were transduced by an Ad vector containing the CA promoter, more than 90% of the cells were transduced. Furthermore, Ad vector-mediated PPAR gamma gene transduction into EBs led to more efficient differentiation into adipocytes than could untransduced EBs, examined in terms of lipogenic enzyme activities and accumulation of the lipid droplets.

Conclusions Ad vector-mediated transduction into EBs could be a valuable tool for molecular switching of cell differentiation and could be applied to regenerative medicine.

Keywords adenovirus vector; embryonic stem cells; embryoid bodies; regenerative medicine

Introduction

Embryonic stem (ES) cells are derived from mammalian blastocysts and maintain pluripotency, an ability to differentiate into all types of somatic and germ cells. Another important property of ES cells is their robust and infinite growth, equivalent to tumor cells in spite of their normal karyotype. Mouse ES (mES) cells were isolated from

mouse blastocysts in 1981 [1] and have been extensively used to generate knockout mice. Human ES cells were established in 1998 [2] and are considered promising sources for cell transplantation therapy.

ES cells differentiate spontaneously *in vitro* in a random fashion into all three germ layers. Therefore, establishment of the differentiation protocols from ES cells into pure target cells is expected to be applicable to regenerative medicine. Among many methods for inducing cellular differentiation from ES cells, genetic manipulation is one of the most powerful techniques to control cellular differentiation. Long-term constitutive gene expression systems such as electroporation methods and a retrovirus vector system by which antibiotic-resistant stable cells are established have been developed and utilized so far to differentiate ES cells into committed cells and to analyze gene function [3–7]. However, such expression systems may be problematic especially in therapeutic application because the transgene is randomly integrated into the host cell genome and this leads to a risk of mutagenesis [8]. Therefore, instead of a long-term constitutive gene expression system, establishment of a transient expression system is required for differentiation from ES cells into functional cells.

Among the various types of gene delivery vectors, adenovirus (Ad) vectors based on human Ad type 5 (hAd5) have been widely used for gene delivery, since they can be amplified at high titers, have the ability to package relatively large-sized foreign DNA, and achieve high transduction efficiency [9,10]. Furthermore, in contrast to stable gene expression, only little genomic DNA of the Ad vector is integrated into the host cell DNA, and its expression is transient. These features of the Ad vector are thought to be advantageous for cellular differentiation since transgene expression is not often needed for the cells after differentiation. From such a viewpoint, we previously reported efficient transduction into mES cells using an Ad vector [11].

When ES cells differentiate into functional cells, they are suspended in the medium on non-adherent culture plates or in hanging drops. The suspended ES cells spontaneously aggregate to form spheres, called embryoid bodies (EBs), which consist of semi-organized tissue including contractile cardiac myocytes and hemoglobin-containing blood islands [12]. Although the procedures to regulate ES cell differentiation are often carried out through EBs [5,7], no study has been performed investigating the transduction efficiency for EBs.

In the present study, we optimized transduction efficiency through comparison of the promoter activities in EBs by using β-galactosidase (LacZ)-expressing Ad vectors. Furthermore, to test whether the differentiation efficiency of functional cells from EBs could be improved by using an Ad vector-mediated gene transfer, we introduced a peroxisome proliferator-activated receptor gamma (PPARγ) gene, which has been shown to be indispensable for adipogenesis [13,14], or a CCAAT/enhancer binding protein alpha (C/EBPα) gene, which has also been shown to be a key transcription factor for adipogenesis [15,16], into EBs.

Materials and methods

Plasmid construction and generation of Ad vectors

Ad vectors were constructed using an improved *in vitro* ligation method [17,18]. The murine PPARγ1 gene, which is derived from pHMCMV6-PPARγ1 (a kind gift from Dr. K. Katayama, Tokyo Metropolitan Institute of Medical Science, Tokyo, Japan) [19], was digested with *Xba*I and *Not*I, and inserted between the *Xba*I and *Not*I sites of pHMCA5 [11], resulting in pHMCA5-PPARγ1. pHMCA5-PPARγ2 was constructed by insertion of the oligonucleotides 5′-catgggtgaaactctgggagattctcctgtagacccagagcatggtgcctt cgctgatgcactgcctatgagcacttcacaagaaattaccatggta-3′ and 5′-taccatggtaatttcttgtgaagtgctcataggcagtgcatcagcgaagg caccatgctctgggtctacaggagaatctcccagagtttcacc-3′ (underlined sequences indicate the mutated *Hinc*II site with silent mutation to prevent cleaving) into the *Nco*I and *Hinc*II sites of pHMCA5-PPARγ1, because murine PPARγ2 cDNA encodes an additional thirty amino acids N-terminal to the first ATG of murine PPARγ1 [20]. Murine C/EBPα cDNA, which is derived from pEF-C/EBPα (a kind gift from Dr. M. Takiguchi, Chiba University, Chiba, Japan) [21], was digested with *Bst*XI, blunted by a Klenow fragment of DNA polymerase, and cloned into the *Pme*I site of pHMCA5, resulting in pHMCA5-C/EBPα. pHMCA5-PPARγ1, pHMCA-PPARγ2, or pHMCA5-C/EBPα was then digested with I-*Ceu*I/PI-*Sce*I and inserted into I-*Ceu*I/PI-*Sce*I-digested pAdHM4 [17], resulting in pAdHM4-CA-PPARγ1, pAdHM4-CA-PPARγ2, or pAdHM4-CA-C/EBPα, respectively.

To generate the virus, Ad vector plasmids were digested with *Pac*I and were then transfected into 293 cells plated in 60 mm dishes with SuperFect (Qiagen, Valencia, CA, USA) following the manufacturer's instructions. The virus was purified by $CsCl_2$ gradient centrifugation, dialyzed with a solution containing 10 mM Tris (pH 7.5), 1 mM $MgCl_2$, and 10% glycerol, and stored in aliquots at −80 °C. The rous sarcoma virus (RSV) promoter, the cytomegalovirus (CMV) promoter, the CMV enhancer/β-actin promoter (CA) promoter, or the human elongation factor-1α (EF-1α) promoter-driven LacZ-expressing Ad vector, Ad-RSV-LacZ, Ad-CMV-LacZ, Ad-CA-LacZ, or Ad-EF-LacZ, respectively, and CA promoter-driven green fluorescent protein (GFP)-expressing Ad vector, Ad-CA-GFP, were constructed previously [11,22]. Determination of virus particles (VP) and biological titer were determined using a spectrophotometric method [23] and by means of an Adeno-X rapid titer kit (Clontech, Palo Alto, CA, USA), respectively. The ratio of the biological-to-particle titer was 1 : 14 for Ad-CA-LacZ, which was re-amplified in 293 cells to use in this study, 1 : 8 for Ad-CA-PPARγ1, 1 : 8 for Ad-CA-PPARγ2, and 1 : 9 for Ad-CA-C/EBPα.

DOI: 10.1002/jgm

Cell culture and EB formation

Mouse E14 ES cells were cultured on mytomycin C-treated mouse embryonic fibroblasts (MEFs) or on a gelatin-coated plate in a leukemia inhibitory factor-containing ES cell culture medium as described previously [11]. To induce formation of EBs, mES cells on MEFs were trypsinized, and MEF layers were separated from mES cells by culturing at 37 °C for 45 min. Nonadherent cells, which contain undifferentiated ES cells, were resuspended in differentiation medium (Dulbecco's modified Eagle's medium (WAKO, Osaka, Japan) containing 15% fetal calf serum (Specialty Media, Inc., Phillipsburg, NJ, USA), 0.1 mM 2-mercaptoethanol (Nacalai tesque, Kyoto, Japan), 1× non-essential amino acid (Specialty Media, Inc.), 1× nucleosides (Specialty Media, Inc.), 2 mM L-glutamine (Invitrogen, Carlsbad, CA, uSA), and penicillin/streptomycin (Invitrogen)) at a concentration of 1×10^5 cells/ml, and 3×10^3 cells were cultured on the inner side of 100 mm Petri dish lids (hanging drop method) and incubated at 37 °C for 2 or 5 days.

Five-day-cultured EBs (5d-EBs) were harvested, washed with phosphate-buffered saline (PBS), and incubated in 1×trypsin/EDTA (Invitrogen) at 37 °C for 5 min. EBs were dissociated in differentiation medium by repeated pipetting and passing through a 20-gauge needle. The single cell suspension was kept on ice for further analysis.

LacZ assay

5d-EBs were transduced with the indicated doses of conventional Ad vectors (Ad-RSV-LacZ, Ad-CMV-LacZ, Ad-CA-LacZ or Ad-EF-LacZ) at 37 °C. Two days later, X-gal staining and β-gal assays were performed as described previously [11]. The EB-derived single cell suspension was transduced with the indicated doses of Ad-CA-LacZ at 37 °C for 1.5 h before plating. The cells were then washed with PBS and plated on gelatin-coated dishes. On the following day, X-gal staining was carried out as described above.

GFP expression analysis

EBs were transduced with the Ad-CA-GFP at 10 000 VP/cell. At 1.5 h after incubation, the cells were washed to remove the Ad vectors and were transferred into fresh medium. The EBs were transduced with 10 000 VP/cell of Ad-CA-GFP three times on days 0, 2, and 5 (hereinafter referred to as triple transduction), as follows: 0d-EBs (ES cells suspension) were transduced with Ad vector in hanging drop for 2 days, and 2d-EBs and 5d-EBs were transduced with Ad vector for 1.5 h. On day 7, GFP fluorescence in the EBs was visualized via confocal microscopy (Leica TCS SP2 AOBS; Leica Microsystems, Tokyo, Japan). The EBs were then trypsinized and analyzed for GFP expression by flow cytometry on a FACSCalibur flow cytometer using CellQuestPro software (Becton Dickinson, Tokyo, Japan)

Adipocyte differentiation with Ad vector

Two days after culture with hanging drop, the EBs were transferred into a Petri dish and maintained for 3 days in suspension culture in differentiation medium containing 100 nM all-*trans*-retinoic acid (RA, WAKO), and then cultured for 2 more days in differentiation medium without RA [24]. The cells were transduced with 10 000 VP/cell of Ad vectors (Ad-CA-LacZ, Ad-CA-PPARγ1, Ad-CA-PPARγ2 or Ad-CA-C/EBPα) at days 0, 2, and 5 as described above and plated on a gelatin-coated dish on day 7. Cells were cultivated in differentiation medium with or without adipogenic supplements (0.1 M 3-isobutyl-L-methylxanthine (Sigma, St. Louis, MO, USA), 100 nM insulin (Sigma), 0.1 μM dexametasone (WAKO), and 2 nM triiodothyronine (Sigma)) and the medium was changed every 2 or 3 days.

Differentiation of EBs into adipocytes was estimated by Oil-red O staining and glycerol-3-phosphate dehydrogenase (GPDH) activity on days 12 and 24 after plating. Oil-red O staining and a GPDH assay were performed using a lipid assay kit and GPDH assay kit, respectively (Cellgarage, Hokkaido, Japan). For the analysis of lipid accumulation, stained lipid was extracted with 100% isopropanol for 5 min and the optical density of the solution was measured at 540 nm. For the GPDH assay, protein content was determined using a Bio-Rad Protein assay kit (Bio-Rad Laboratories, Hercules, CA, USA) employing bovine serum albumin as a standard, and GPDH activities were then normalized to protein content.

Western blotting

ES cells, 2d-EBs, and 5d-EBs were lysed in lysis buffer (20 mM Tris-HCl (pH 8.0), 137 mM NaCl, 1% Triton X-100, 10% glycerol) containing protease inhibitor cocktail (Sigma). Lysates (20 μg) were subjected to sodium dodecyl sulfate/polyacrylamide gel electrophoresis (SDS-PAGE) on 12.5% polyacrylamide gel and transferred onto a polyvinylidene fluoride membrane (Millipore, Bedford, MA, USA). After blocking with 3% skimmed milk in Tris-buffered saline containing 0.1% Tween 20 at room temperature for 2 h, the membrane was incubated with goat anti-CXADR (coxsackievirus and adenovirus receptor, hereinafter referred to as CAR) antibody (R&D Systems, Minneapolis, MN, USA, diluted 1:1000) or mouse anti-Oct-3/4 antibody (Santa Cruz Biotechnology, Inc., Santa Cruz, CA, USA, diluted 1:200) at 4 °C overnight, followed by horseradish peroxidase conjugated anti-goat IgG (Chemicon, Temecula, CA, USA) or anti-mouse IgG (Cell Signaling Technology, Beverly, MA, USA), respectively, at room temperature for 1 h. The band

DOI: 10.1002/jgm

was visualized by ECL Plus Western blotting detection reagents (Amersham Bioscience, Piscataway, NJ, USA) and the signals were read using a LAS-3000 imaging system (FUJIFILM, Tokyo, Japan). For the detection of internal control, a monoclonal anti-β-actin antibody (Sigma, diluted 1 : 5000) and a horseradish peroxidase conjugated anti-mouse IgG were used.

Reverse-transcription polymerase chain reaction (RT-PCR)

Total RNA was isolated as described previously [11]. DNaseI-treated samples were reverse-transcribed using SuperScript II (Invitrogen), and PCR was then performed using KOD Plus DNA polymerase (Toyobo, Osaka, Japan). The PCR conditions were 94 °C for 2 min, followed by appropriate cycles of 94 °C for 15 s, 55 °C for 30 s with 68 °C for 30 s and a final extension of 68 °C for 1 min, except for the addition of 5% dimethyl sulfoxide in the case of C/EBPα and leptin cDNA amplification. PCR products were visualized by ethidium bromide staining after being separated on 2% agarose gel. The sequences and references of primers were as follows: PPARγ(F), 5′-CCCTGGCAAAGCATTTGTAT-3′; PPARγ(R), 5′-AATCCTTGGCCCTCTGAGAT-3′; C/EBPα(F), 5′-CGCTGGTGATCAAACAAGAG-3′; C/EBPα(R), 5′-GTCACTGGTCAACTCCAGCA-3′; aP2(F), 5′-TGGAAGCTTGTCTCCAGTGA-3′; aP2(R), 5′-ACACATT CCACCACCAGCTT-3′; adiponectin(F), 5′-GTTGCAAG CTCTCCTGTTCC-3′; adiponectin(R), 5′-GCTTCTCCAGG CTCTCCTTT-3′; leptin(F), 5′-TGACACCAAAACCCTCA TCA-3′; leptin(R), 5′-CTCAAAGCCACCACCTCTGT-3′, CAR, Oct-3/4, Nanog, Brachyury T, GAPDH and LacZ were described previously [11,25].

Results

Transgene expression in EBs by Ad vectors

Initially, we characterized the EBs used in this study by examining the expression of cellular marker genes. Consistent with previous reports, the expression of Nanog and Oct-3/4, both of which are transcription factors involved in the maintenance of pluripotency in mES cells, were down-regulated following EB formation, whereas the expression of brachyury T, the early pan-mesodermal marker, was detectable in EBs (Figures 1A and 1B) [26,27]. It is known that expression of CAR, a primary receptor of Ad, is essential for Ad vector-mediated gene transduction [10]. To confirm whether EBs could be efficiently transduced with Ad vectors, we assessed the expression of CAR in EBs (Figures 1A and 1B). We found that expression levels of CAR in both 2d-EBs and 5d-EBs (EBs cultured for 2 or 5 days, respectively) were similar to those of mES cells, suggesting that exogenous genes could be introduced into EBs by using a conventional Ad vector.

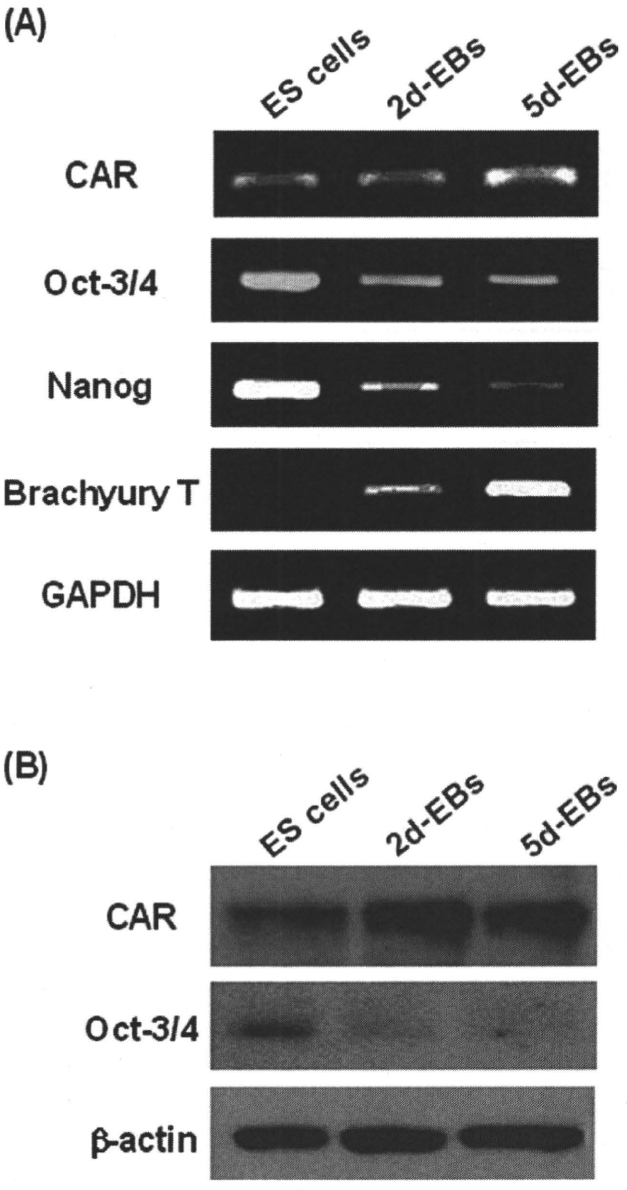

Figure 1. RT-PCR and Western blot analysis of ES cells and EBs. Total RNA or whole cell lysates were isolated from ES cells (lane 1), 2d-EBs (lane 2), or 5d-EBs (lane 3). RT-PCR (A) and Western blotting (B) were carried out as described in Materials and Methods. Abbreviations: ES cells, embryonic stem cells; EBs, embryoid bodies; 2d-EBs, two-day-cultured EBs; 5d-EBs, five-day-cultured EBs; CAR, coxsackievirus and adenovirus receptor

We next prepared LacZ-expressing Ad vectors under the control of four different promoters, the RSV promoter, the CMV promoter, the CA promoter, or the EF-1α promoter (Ad-RSV-LacZ, Ad-CMV-LacZ, Ad-CA-LacZ, or Ad-EF-LacZ, respectively) to optimize the efficiency of transgene expression in EBs. 5d-EBs were transduced with each Ad vector (3000 virus particles (VP)/cell) and LacZ expression in the cells was measured. As shown in Figures 2A and 2B, Ad-CA-LacZ-transduced EBs showed

DOI: 10.1002/jgm

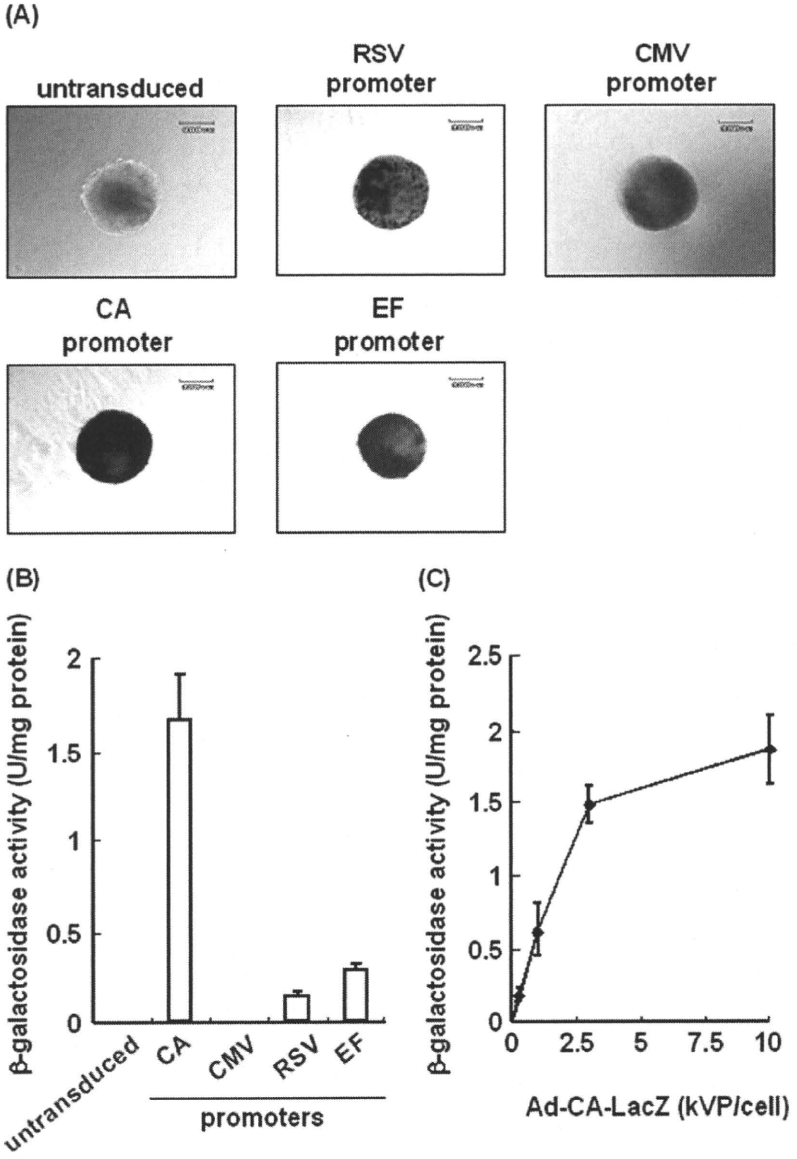

Figure 2. Ad vector-mediated transduction efficiency in EBs as determined using various types of promoters. 5d-EBs were transduced with Ad vectors at 3000 VP/cell for 2 days. After 48 h, X-gal staining (A) and β-galactosidase luminescence assay (B) were performed as described in Materials and Methods. Similar results for X-gal staining were obtained in five independent experiments. (C) 5d-EBs were transduced with 300, 1000, 3000, or 10 000 VP/cell of Ad-CA-LacZ for 2 days. Two days after transduction, LacZ expression in the cells was measured by luminescence assay. The data (B and C) are expressed as mean ± standard deviation (S.D.) (n = 3). Abbreviations: RSV, rous sarcoma virus; CMV, cytomegalovirus; CA, CMV enhancer/β-actin promoter; EF-1α, human elongation factor-1α

greater LacZ expression than did Ad-RSV-LacZ- or Ad-EF-LacZ-transduced EBs. Although the CMV promoter is in wide use in transduction experiments, Ad-CMV-LacZ-transduced EBs showed little expression of LacZ. These data indicate that the transduction efficiency in EBs is dependent on the promoter and that the CA promoter is the most active in EBs among the four types of promoters examined in this study.

To determine an appropriate dose of Ad-CA-LacZ for the transduction efficiency in EBs, 5d-EBs were transduced with a different dose of Ad-CA-LacZ for 2 days, and then LacZ production in the cells was quantified by means of a luminescence assay. The expression of LacZ in the EBs increased depending on the dose of Ad vectors and reached a plateau at 3000–10 000 VP/cell (Figure 2C). To obtain high transgene expression, the concentration of Ad vector with 10 000 VP/cell was employed for further analysis. Next, we examined whether an increase in the efficiency of LacZ expression could be obtained in EBs by using fiber-modified Ad vectors. We generated Ad-RGD-CA-LacZ and AdK7-CA-LacZ, which contain the Arg-Gly-Asp (RGD) peptide in the HI loop of the fiber knob [28] and seven tandem lysine residues (K7) in the C-terminal of the fiber knob [29], respectively. These Ad vectors transduce cells through αv integrin and heparan sulfates, respectively, even if cells lack CAR expression. 5d-EBs were transduced with 1000, 3000, or 10 000 VP/cell of Ad-CA-LacZ, AdRGD-CA-LacZ, or

DOI: 10.1002/jgm

AdK7-CA-LacZ for 2 days and a luminescence assay for the measurement of LacZ expression was performed. The amount of LacZ expression obtained by using fiber-modified Ad vectors was comparable to that obtained by using a conventional Ad vector (data not shown). Thus, these results indicate that the conventional Ad vector containing the CA promoter is the most suitable vector for transduction to EBs.

Next, 5d-EBs were transduced with 10 000 VP/cell of CA promoter-driven GFP-expressing Ad vector, Ad-CA-GFP, to examine whether transgene expression could be observed inside the EBs. Confocal microscopic analysis revealed GFP expression only at the periphery of the EBs (Figure 3A, middle). The percentage of GFP-expressing cells in the EBs was $25.3 \pm 2.3\%$ as determined by flow cytometric analysis (Figure 3B, middle). A similar pattern of transgene expression was observed in the X-gal staining of sliced sections of EBs transduced with Ad-CA-LacZ (data not shown). These results suggest that Ad vectors do not transduce the cells in the interior of EBs because of the physical barrier constituted by their tight connection. Therefore, repeated transduction of Ad vectors was attempted to express the transgene in the EB interior. First, a transgene was introduced into mES cells but not EBs by Ad vector in hanging drop. After transduction into ES cells under the hanging drop, the 2d-EBs and 5d-EBs were transduced with Ad vector again. Thus, the EBs were transduced with Ad vector three times in total (triple transduction: see Materials and Methods). When the EBs were transduced with Ad-CA-GFP by triple transduction, GFP expression was observed even in the interior of the EBs at day 7, although not all the EB cells showed GFP expression (Figure 3A, right). Furthermore, flow cytometric analysis showed that the GFP-positive cells were significantly increased to $39.2 \pm 4.3\%$ ($p < 0.05$ vs. single infection) (Figure 3B, right), although the transduced cells would be diluted due to their cell division. When the number of cells composed of 7d-EBs was measured, there was almost no difference in cell numbers between untransduced EBs and GFP-transduced EBs by triple transduction (data not shown). In addition, 7d-EBs transduced with Ad vector by triple transduction as well as untransduced EBs could differentiate into adipocytes (Figures 4 and 5), showing that Ad vectors have no cytotoxicity to EBs. These results indicate that triple transduction by using Ad vector is effective to express the transgene in the interior of EBs.

As reported previously, hematopoietic differentiation from ES cells via EBs has been usually performed using an EB-derived single cell [7]. To investigate whether the Ad vector was able to be efficiently introduced into EB-derived single cells, EB-derived single cells, which were obtained by typsinization of 5d-EBs, were transduced with Ad-CA-LacZ (Figure 3C). LacZ expression in the EB-derived single cells was dose-dependent, and more than 90% of the cells expressed LacZ at 3000 VP/cell, demonstrating that the EB-derived single cells efficiently expressed LacZ by transduction using Ad vector containing the CA promoter.

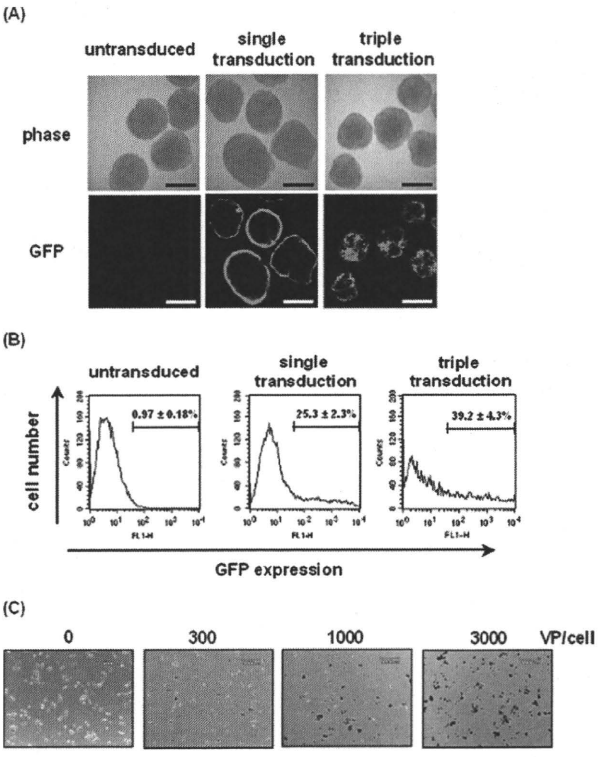

Figure 3. Optimization of gene transfer into EBs by Ad vector. EBs were transduced with 10 000 VP/cell of Ad-CA-GFP by single transduction (A, B; middle) or triple transduction (A, B; right). On day 7, (A) confocal microscopic analysis and (B) flow cytometric analysis were performed. The data are expressed as mean ± S.D. (n = 5). Untransduced EBs are represented as a negative control (A, B; left). Scale bar indicates 300 μm. (C) 5d-EB-derived single cells obtained by trypsin treatment of 5d-EBs, were transduced with Ad-CA-LacZ at doses of 0, 300, 1000, or 3000 VP/cell. On the following day, X-gal staining was performed. Similar results were obtained in three independent experiments. Scale bar indicates 200 μm. Abbreviation: GFP, green fluorescent protein

Regulation of cellular differentiation using Ad vector-mediated gene delivery

To confirm that Ad vector-mediated transduction was applicable to basic research or regenerative medicine, we introduced functional genes, which regulate cellular differentiation, into EBs. As a model for cellular differentiation, EBs were differentiated into adipocytes by using Ad vector-mediated transduction of an adipogenesis-related gene. We constructed three Ad vectors, Ad-CA-PPARγ1, Ad-CA-PPARγ2, and Ad-CA-C/EBPα, which expressed murine PPARγ1, PPARγ2, and C/EBPα, respectively. PPARγ and C/EBPα have been shown to play essential roles in adipogenesis [13–16,30]. PPARγ is present in two isoforms, PPARγ1 and PPARγ2, generated by alternative promoter usage [20]. PPARγ2 has an additional thirty N-terminal amino acids relative to PPARγ1. We used both PPARγ1 and PPARγ2 since both could drive a full program of adipogenesis in cultured PPARγ-deficient cells [31]. No study has directly compared the adipogenesis ability, especially adipocyte differentiation from mES cells, of PPARγ1, PPARγ2, and C/EBPα.

DOI: 10.1002/jgm

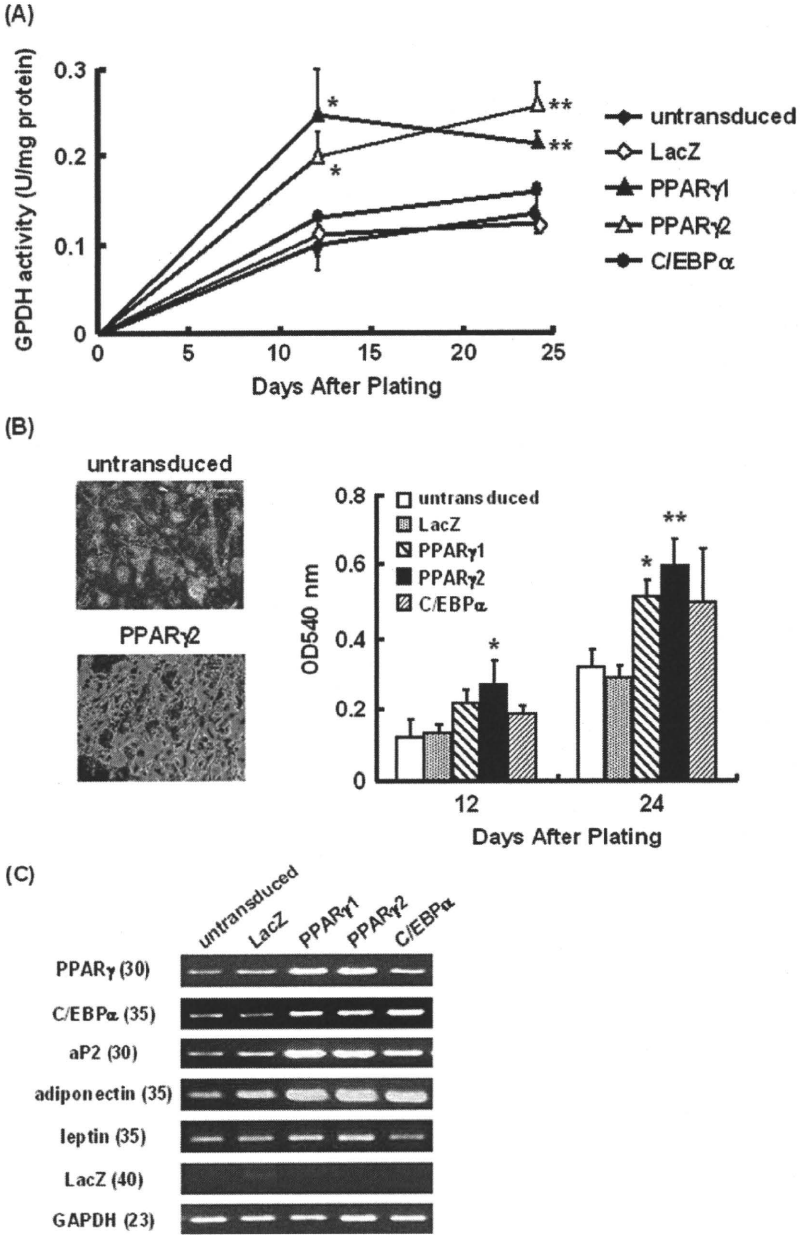

Figure 4. Efficient adipocyte differentiation from EBs by Ad vector-mediated PPARγ gene transfer. EBs were transduced in triplicate with 10 000 VP/cell of Ad-CA-LacZ, -PPARγ1, -PPARγ2, or -C/EBPα. After plating onto a gelatin-coated dish on day 7, EBs were cultured for 24 days with adipogenic supplements. On days 12 and 24 after cultivation GPDH activity in the cell was measured (A). The data are expressed as mean ± S.D. (n = 4). (B) Lipid accumulation was detected by Oil-red O staining at day 24 in the untransduced cells (left, top) or PPARγ2-expressing cells (left, bottom). Scale bar indicates 60 μm. After staining with Oil-red O, stained lipid was extracted and the absorbance at 540 nm was measured (right). The data are expressed as mean ± S.D. (n = 4). (C) The expression of PPARγ, C/EBPα, aP2, adiponectin, leptin, and GAPDH was measured by semi-quantitative RT-PCR. The primer for PPARγ amplified both PPARγ1 and PPARγ2. Cycle number is indicated in parentheses. *$p < 0.05$ and **$p < 0.01$, respectively, as compared with untransduced EBs. Abbreviations: GPDH, glycerol-3-phosphate dehydrogenase; PPARγ, peroxisome proliferator-activated receptor gamma; C/EBPα, CCAAT/enhancer binding protein alpha

The procedure for adipocyte differentiation from mES cells was carried out as reported by Dani *et al.* [24] except for the step of Ad vector-mediated gene transfer. First, 7d-EB-derived single cells, which were prepared by trypsinization of 7d-EBs, were transduced with Ad-CA-LacZ, -PPARγ1, -PPARγ2, or -C/EBPα because Ad vectors could efficiently introduce a transgene into EB-derived single cells, as shown in Figure 3C. Then, to estimate adipocyte differentiation, GPDH activities in the cells were measured after 24 days cultivation with adipogenic supplements. Although PPARγ-transduced cells exhibited a high level of GPDH activity compared to untransduced cells or LacZ-transduced cells, it was approximately 50-fold lower than that of the untransduced sphere form of EBs, which had not been obtained by trypsin treatment, but was cultured in differentiation medium with adipogenic supplements (data not shown). It is possible that cell-cell interaction in the sphere form of EBs

DOI: 10.1002/jgm

might be essential for adipocyte differentiation from ES cells, and this might be why trypsinized EBs showed lower differentiation. Therefore, EBs in the sphere form were then treated with each Ad vector by triple transduction, and GPDH activity was measured after cultivation with adipogenic supplements. The levels of GPDH activity in the cells transduced with Ad-CA-LacZ or Ad-CA-C/EBPα were similar to those of untransduced EBs. On the other hand, it was significantly increased by Ad vector-mediated PPARγ (PPARγ1 and PPARγ2) expression at days 12 and 24 (Figure 4A). Moreover, Oil-red O staining revealed that 70–80% of the cells transduced with PPARγ were Oil-red O positive, whereas 50–60% were LacZ- or C/EBPα-transduced cells or untransduced cells (data not shown). In particular, many large lipid droplets accumulated in the cells transduced with Ad-CA-PPARγ1 or Ad-CA-PPARγ2 compared to untransduced EBs (Figure 4B, data not shown). We also confirmed the expression of marker genes of adipocyte differentiation by semi-quantitative RT-PCR analysis. As shown in Figure 4C, PPARγ, C/EBPα, adipocyte-specific fatty acid binding protein (aP2), and adiponectin expression were up-regulated in PPARγ1- and PPARγ2-transduced EBs (Figure 4C). Furthermore, when we measured the expression levels of LacZ mRNA to examine whether Ad vector-mediated transduction still continued, its expression was undetectable in Ad-CA-LacZ-transduced EBs (Figure 4C), suggesting that expression of PAPRγ or C/EBPα, which was observed in PPARγ- or C/EBPα-transduced EBs, would not be derived from the Ad vector but from endogenous genes.

Next, we examined whether Ad vector-mediated transduction into EBs could increase the differentiation efficiency even in the absence of adipogenic supplements. Adipogenesis from EBs was promoted by transduction of PPARγ, although the levels of GPDH activity and lipid droplet accumulation could not achieve the adipogenic supplements-treated levels (Figure 5 and data not shown). These results indicate that Ad vector-mediated transduction of the PPARγ gene into EBs could improve the efficiency of adipocyte differentiation from ES cells with or without adipogenic supplements.

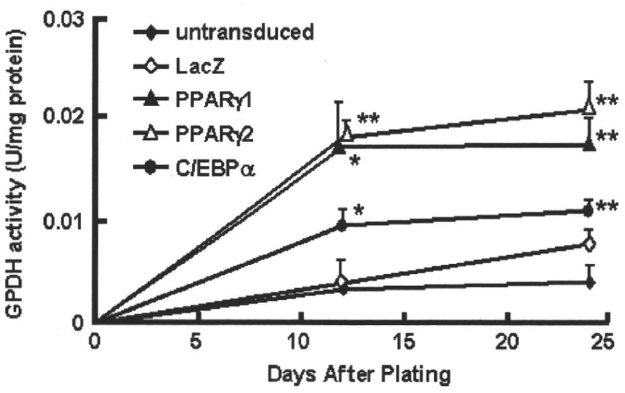

Figure 5. Ad vector-mediated transduction into EBs promotes adipogenesis in the absence of adipogenic supplements. EBs were transduced in triplicate with 10 000 VP/cell of each Ad vector, and then GPDH activity was measured after cultivation in differentiation medium without adipogenic supplements. The data are expressed as mean ± S.D. (n = 3). *$p < 0.05$ and **$p < 0.01$, respectively, as compared with untransduced EBs

Discussion

In the present study, we compared the transduction efficiency of four types of promoters (RSV, CMV, CA, and EF-1α), which are widely used in transduction experiments, in EBs by using Ad vector, and demonstrated that the CA promoter could robustly drive transgene expression in EBs (Figures 2A and 2B). We concluded that the CA promoter was the most appropriate promoter for transduction into EBs. We also showed that in trypsinized EBs, more than 90% of the cells were transduced with the Ad vector containing the CA promoter, and that a transgene could be successfully expressed in the interior of EBs by triple transduction (Figure 3). We and other groups have demonstrated that the CA promoter is potentially active in mES cells [11,32], human $CD34^+$ cells [33,34], and embryos of transgenic mice [35], suggesting that the CA promoter is active particularly in immature cells including stem cells. EBs are thought to be composed of immature cells because of the presence of Oct-3/4 and Nanog, although their expression levels are moderate (Figure 1). Thus, the CA promoter is useful in attaining high levels of transgene expression in EBs. Interestingly, the CMV promoter, which is one of the strongest promoters known so far, had little activity not only in mES cells [11,32], but also in EBs (Figures 2A and 2B). This might be due to the defense response against the transcription of foreign genes using a non-cellular promoter in immature cells. Rust *et al.* [36] reported that the CMV promoter was active in cardiac myocytes derived from mES cells in spite of being inactive in undifferentiated ES cells. These results suggest that the CMV promoter, in contrast to the CA promoter, does not work in both EBs and ES cells, and it is possible that transcriptional silencing might occur through some mechanism such as the DNA methylation of the CMV promoter [37]. However, Rufaihah *et al.* recently showed that about 90% of the human 7d-EB-derived single cells were transduced with an Ad vector containing the CMV promoter [38]. Although it is unknown why the CMV promoter has potent activity in human EBs, the transcriptional silencing using the CMV promoter might occur in murine but not human cells. Thus, the silencing mechanism in the CMV promoter in immature cells should be further investigated.

Differentiation procedures from ES cells by gene delivery have been performed using long-term constitutive expression systems such as those involving retrovirus vector [4,7]; however, these procedures might be not suitable for therapeutic use. Ad vectors could be useful because of their transient expression. However, few studies have been performed to differentiate ES cells into functional cells using transient expression systems. In the

DOI: 10.1002/jgm